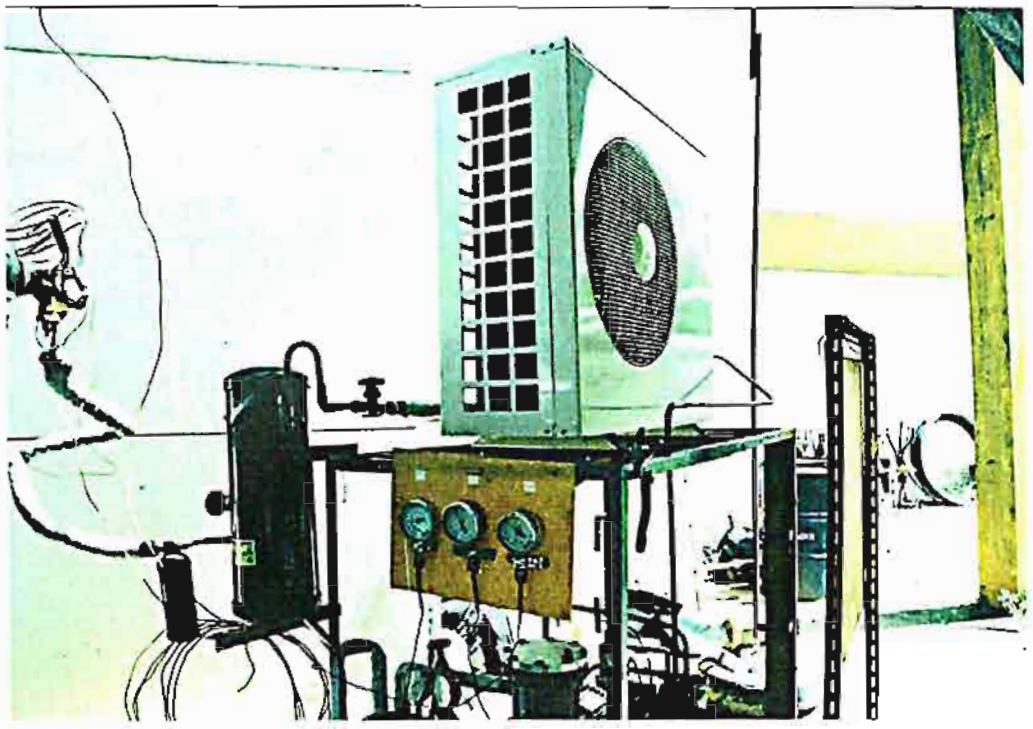

C.5 Condensing unit

C.6 Ice storage tank

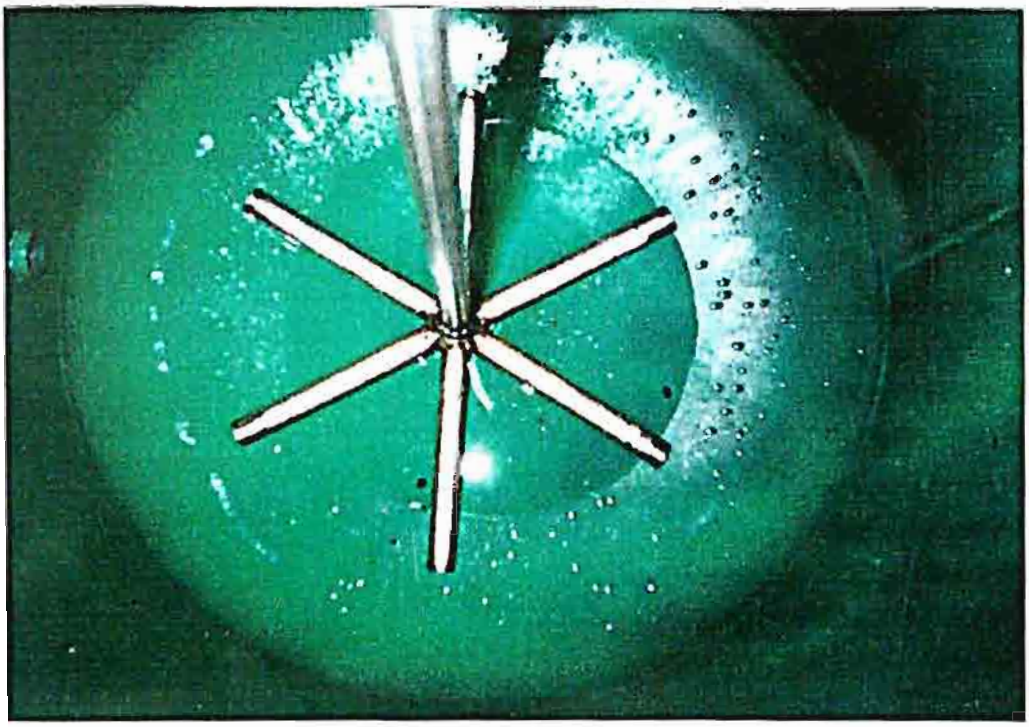

C.7 Nozzle

C.8 Produced ice in the storage tank

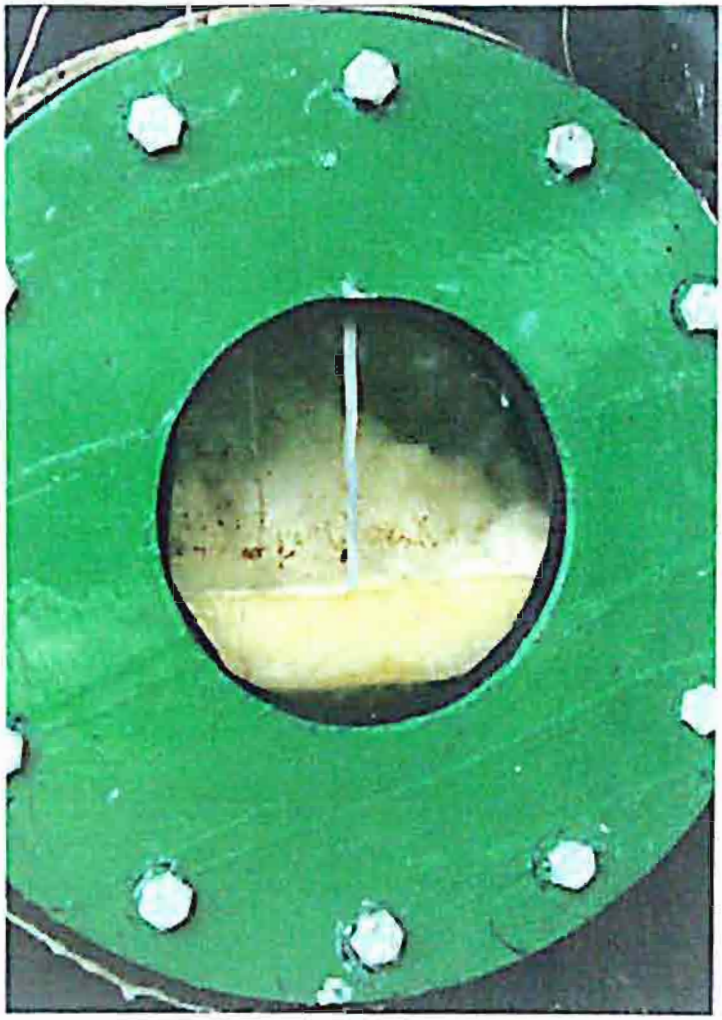

C.9 Produced ice in the storage tank

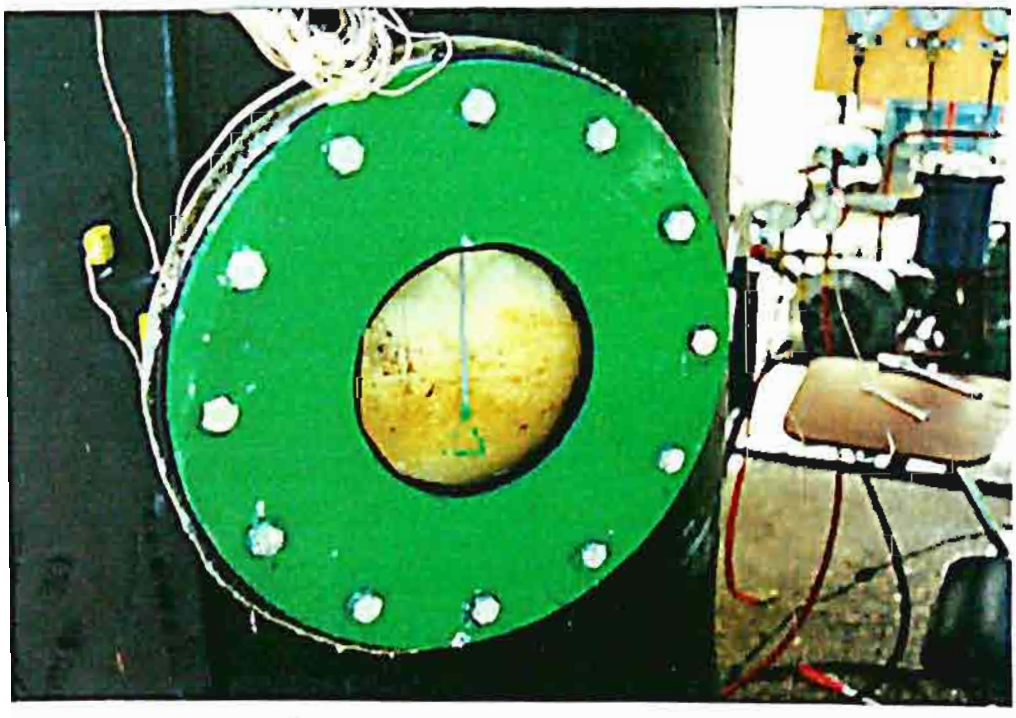

C.10 Produced ice in the storage tank

APPENDIX D

Published Papers

APPENDIX D

Published Papers

1. Energy Analysis of an Ice Thermal Energy Storage Prototype with Direct Contact Evaporator, Energy-The International Journal, Submitted.
2. Heat Transfer Model of a Direct a Direct Contact Evaporator, Applied Energy, Submitted.
3. Feasibility of Using Ice Thermal Energy Storage with Direct Contact Evaporator in an Office Building, Energy Research-The International Journal, Submitted.

Energy Analysis of an Ice Thermal Energy Storage Prototype with Direct Contact Evaporator

N. Vorayos
The Joint Graduate School of Energy and Environment,
King Mongkut's University of Technology Thonburi,
Bangkok 10140, Thailand
A. Nuntaphan, S. Seewattanangkoon and T. Kiatsiriroat
Department of Mechanical Engineering, Chiang Mai University,
Chiang Mai 50200, Thailand

Abstract – In this research, an ice thermal energy storage with direct contact evaporator has been studied and is applied in an office room. The system consists of two processes, air conditioning process and ice storage. The storage has another refrigeration unit and is designed as a partial storage type. From the experimental data, the mathematical models for main components of each process which are compressor, condenser, expansion valve, water chiller and direct contact evaporator are developed and the system simulation is created. From the result, it could be shown that the simulation agrees well with the experiment. From the simulation, it indicates that the appropriate capacity of the ice thermal energy storage system which is 8 kW can shift 48.7 % of peak cooling load from on-peak to off-peak period. Moreover, under this condition, 27% of operating cost are saved comparing to those of the conventional system.

Keywords: Ice thermal energy storage system, direct contact heat transfer, system simulation

Submitted to **Energy – The International Journal,**

Address of Correspondence and proof:
Prof. Dr. Tanongkiat Kiatsiriroat
Department of Mechanical Engineering, Faculty of Engineering,
Chiang Mai University, Chiang Mai 50200, Thailand.
Tel:6653-944144 Fax:6653-944145 E-mail: *tanong@dome.eng.cmu.ac.th*

1. INTRODUCTION

As electricity demand in commercial building is mainly caused by cooling system, ice hermal energy storage (ITES) is a concept that is becoming more attractive to reduce the)perating cost of the building in both of demand and energy charges [1-3]. Demand and energy :harges are based on the peak power consumption during a peak hour and the total energy 'onsumed respectively. The ITES technique shifts the cooling load from peak to off-peak by unning the air

conditioning compressor during the off-peak hour when the energy cost is the lowest to produce :e stored in the storage tank. Water from this tank is circulated for the cooling purpose during ıe on-peak hour. At present, most of the ITES systems used are the ice-on-coil storage system ·f which the ice is formed directly on the coils submerged in the water. There are two main ·roblems, big space for handling the evaporator coil is needed and high thermal resistance is ·btained due to the low thermal conductivity of the ice when it is formed on the coil [4-5].)uring the ice formation process, as the ice thickness is increased, the rate of heat extraction ecreases. Thus, the direct contact heat transfer technique has been much interest in recent years hrough its application to overcome these problems [6-7]. In this paper, an application of an ice hermal energy storage with the direct contact evaporator system for air-conditioning of an office n Chiang Mai, Thailand has been carried out. The mathematical models of the main components n both of air-conditioning and direct-contact ITES system have been developed and the)erformance analysis of the whole system has been investigated.

2. THE AIR-CONDITIONING SYSTEM

The air-conditioning system with the ITES unit used in this work are shown schematically in Fig. 1.

The system consists of two main cycles, chilled water cycle and ice storage cycle. The ITES or ice storage cycle is designed as a partial storage type and the whole system uses R12 refrigerant as the working fluid. During the off-peak period the ice storage cycle is operated to proceed the ice formation process. The ice is stored in the storage tank. During the on-peak hours, chilled water cycle is operated to produce the cooled water to achieve the cooling requirement. The cooled water passes from the chiller to the fan-coil unit to exchange heat and then turns back to the chiller. If the required cooling load is higher than the capacity of the chiller, the chilled water from the fan-coil unit controlled by a two-way valve will pass through the ice storage tank to lower the chilled water temperature before going back to the chiller.

An air conditioning unit is operated to support cooling load of a selected office in Chiang Mai city. The area of the office is 71.5 m^2 of which the maximum peak cooling load gained on the designed day in April is approximately 18 kW.

In this study, modeling equations, which describe the behavior of the main system components have been investigated and the system simulation has been carried out to find out the appropriate size of the ITES.

3. MATHEMATICAL MODEL

In this section, the mathematical models of the main components for the air conditioner including the direct contact ITES could be described as follows:

3.1 Chilled Water Refrigeration Cycle

For chilled-water refrigeration cycle, a standard vapor-compression refrigeration system is simulated under steady-state conditions to produce the chilled water for supporting the cooling load. In this case, the chilled water cycle is operated as a base cycle. The compressor is usually worked at constant full speed. Thus, modeling of each component could be developed at various refrigerant mass flow rates. The details have been described as follows:

Compressor Modeling

Kiatsiriroat et al. [8] generates a mathematical model of a reciprocating compressor, which is modified from Stoecker [9] as

$$\frac{P_{cp,i}}{P_{cp,o}} = f\left(\frac{m_r T_{cp,i}^{0.5}}{P_{cp,i}}, N\right), \tag{1}$$

or

$$\frac{P_{cp,i}}{P_{cp,o}} = f\left(\frac{m_r T_{cp,o}^{0.5}}{P_{cp,o}}, N\right), \tag{2}$$

where N is the compressor speed in rps, m_r is the refrigerant mass flow rate in kg/s, $T_{cp,i}$, $T_{cp,o}$, $P_{cp,i}$ and $P_{cp,o}$ are temperatures and pressures at the inlet and outlet ports of the compressor in K and MPa, respectively.

With the experimental results from Figs. 2 and 3, the relations in Eqs. (1) and (2) can be characterized as

$$\frac{P_{cp,i}}{P_{cp,o}} = 0.0973\left(\frac{m_r T_{cp,i}^{0.5}}{P_{cp,i}}\right) + 0.0663, \tag{3}$$

and

$$\frac{P_{cp,i}}{P_{cp,o}} = -0.0057\left(\frac{m_r T_{cp,o}^{0.5}}{P_{cp,o}}\right)^2 + 0.0936\left(\frac{m_r T_{cp,o}^{0.5}}{P_{cp,o}}\right) + 0.1071. \tag{4}$$

Moreover, the pressure ratio of the compressor could also be calculated from

$$\frac{P_{cp,i}}{P_{cp,o}} = \left(\frac{T_{cp,i}}{T_{cp,o}}\right)^{k/(k-1)} \tag{5}$$

where k is the polytropic index depending on the refrigerant mass flow rate as

$$k = f(m_r). \tag{6}$$

From the experiments, the relations between these two parameters can be expressed as shown in Fig. 4 which is

$$k = 0.2216 m_r + 1.1949. \tag{7}$$

Condenser Modeling

In this work a counter flow heat exchanger having circulating water as a coolant is used to extract heat from the refrigeration system. From the experiment, it could be found that the refrigerant becomes saturated liquid after passing the condenser. The heat extracted can be calculated from

$$Q_{cd} = m_r\left(h_{cd,i} - h_{cd,o}\right). \tag{8}$$

Q_{cd} is the rate of heat extraction, $h_{cd,i}$ and $h_{cd,o}$ are the enthalpies at the inlet and the outlet of the condenser, respectively.

Expansion Valve Modeling

The expansion valve is operated manually to control the refrigerant mass flow and the pressure of the cycle. From the results as shown in Fig. 5, it could be found that the pressure ratio at the valve depends on the refrigerant mass flow rate where

$$\frac{P_{ex,o}}{P_{ex,i}} = f(m_r), \tag{9}$$

and the characteristic equation at the valve can be experimentally expressed as

$$\frac{P_{ex,o}}{P_{ex,i}} = -20.114m_r^2 + 3.5432m_r + 0.1291. \tag{10}$$

Chiller Modeling

The water chiller in this case is a counter flow type and the heat transfer rate could be calculated from

$$Q_{ch} = m_r(h_{ch,o} - h_{ch,i}), \tag{11}$$

or

$$Q_{ch} = m_w C_{cpw}(T_{w,i} - T_{w,o}), \tag{12}$$

and

$$Q_{ch} = (UA)_{ch}\left[\frac{(T_{w,i} - T_{ch,o}) - (T_{w,o} - T_{ch,i})}{\ln\left[\frac{T_{w,i} - T_{ch,o}}{T_{w,o} - T_{ch,i}}\right]}\right]. \tag{13}$$

From the experiments, it could be found that there is a pressure drop across the condenser and the chiller, and it is expressed in terms of the pressure ratios at the expansion valve and compressor as

$$\frac{P_{cp,i}}{P_{cp,o}} = -4.6771\left[\frac{P_{ex,o}}{P_{ex,i}}\right]^2 + 3.1933\left[\frac{P_{ex,o}}{P_{ex,i}}\right] - 0.33. \tag{14}$$

3.2 Ice Storage Refrigeration Cycle

For the ice storage system, another standard vapor compression refrigerant cycle is operated to produce ice. R12 is injected through the expansion valve into the water in the direct contact evaporator/storage tank directly to extract heat. The diagram of the system is shown in Fig. 6.

Compressor Modeling

During the ice producing, the compressor model could be characterized similar to that of the chilled water system. From the results as shown in Figs. 7 and 8, the characteristic equation of the compressor can be expressed as

$$\frac{P_{cp,i}}{P_{cp,o}} = \left[\begin{array}{l}\left(0.0027N^2 - 0.0705N + 0.3297\right)\left[\dfrac{m_r T_{cp,o}^{0.5}}{P_{cp,o}}\right]^2 \\ +\left(-0.0013N^2 + 0.028N + 0.1428\right)\left[\dfrac{m_r T_{cp,o}^{0.5}}{P_{cp,o}}\right] \\ +\left(0.0026N^2 - 0.0685N + 0.6253\right)\end{array}\right], \tag{15}$$

and

$$k = 1.7525m_r + 1.1571. \tag{16}$$

Condenser Modeling

In this case, a cross flow heat exchanger having air circulating as a coolant is used to extract heat from the refrigerant. The temperature ratio could be characterized as

$$\frac{T_{a,o}-T_a}{T_{cd,i}-T_a}=f\left(\frac{(UA)_{cd}}{m_a C_{pa}}\right). \tag{17}$$

From the experiments as shown in Fig. 9, the characteristic equation of the condenser can be expressed as

$$\frac{T_{a,o}-T_a}{T_{cd,i}-T_a}=\frac{0.2723(UA)_{cd}}{m_a C_{pa}}+0.0107. \tag{18}$$

Expansion Valve Modeling

The characteristic equation of the expansion valve similar to Eqn. (9) can be expressed from the results shown in Fig. 10 as

$$\frac{P_{ex,o}}{P_{ex,i}}=\begin{bmatrix}\left(0.4839N^2-12.657N+59.808\right)m_r^2\\+\left(-0.0252N^2+0.5546N+0.9465\right)m_r\\+\left(0.0031N^2-0.0783N+0.6857\right)\end{bmatrix}. \tag{19}$$

As shown in Fig. 6, there are some accessory components in this system such as filter drier, accumulator and receiver. These components cause the pressure drops and heat losses also occur. From the experiments, the pressure drop related to the pressure ratio of the compressor and the expansion valve can be expressed as

$$\frac{P_{cp,i}}{P_{cp,o}}=0.954\left(\frac{P_{ex,o}}{P_{ex,i}}\right). \tag{20}$$

Moreover, it could be found that there is pressure drop across the condenser and it could be expressed as

$$P_{cd,o} = P_{cd,i} - 0.034. \tag{21}$$

Direct Contact Evaporator Modeling

Kiatsiriroat et al [7] generated a mathematical model for a direct contact evaporator by using lump model. The thermal characteristics of the water in the tank analyzed by the energy balance could be expressed as

$$\frac{d}{dt}(M_w h_w) + M_t C_t \frac{dT}{dt} = m_r(h_{ev,i} - h_{ev,o}) + (UA)(T_a - T_w). \tag{22}$$

As shown in the equation, the first three terms relate to the enthalpy change rates of the water, the container and the refrigerant, respectively. The last term relates to the external heat gain from the surrounding ambient. In this study, the direct contact evaporator is well insulated, the heat gain could be neglected. Then, the water temperature of the water inside the tank is separately considered in two processes, which are sensible heat process and ice formation process. The characteristic equations of the direct contact evaporator during the sensible heat process and the ice formation process can be expressed in the following equations, respectively as

$$T_w^* = T_w + \frac{m_r(h_{ev,i} - h_{ev,o})\Delta t}{M_t C_{pt} + M_w C_{pw}} \tag{23}$$

$$M_{ice} = \frac{m_r(h_{ev,o} - h_{ev,i})\Delta t}{L} \tag{24}$$

Due to the long length of the pipes between the evaporator unit, the compressor and the condenser in the direct contact experiment set-up, the heat gain and loss are considered. From the preliminary study, the heat gain between the low temperature refrigerant flowing inside the pipes from the evaporator to the compressor and the surrounding ambient can be characterized as

$$m_r C_{pr}\left(T_{cp,i} - T_{ev,o}\right) = f\left(T_a - \left(\frac{T_{ev,o} + T_{cp,i}}{2}\right), m_r\right) \tag{25}$$

From the experiments, the equation can be expressed as

$$m_r C_{pr}\left(T_{cp,i} - T_{ev,o}\right) = \left[\begin{array}{l} \left(-0.0459 m_r^2 + 0.0005 m_r + 0.0003\right)\left(T_a - \left(\frac{T_{ev,o} + T_{cp,i}}{2}\right)\right)^2 \\ + \left(0.9138 m_r^2 + 0.1596 m_r + 0.0356\right)\left(T_a - \left(\frac{T_{ev,o} + T_{cp,i}}{2}\right)\right) \\ + \left(2.663 m_r^2 + 1.1131 m_r - 0.1304\right) \end{array}\right]. \tag{26}$$

Then, for the high temperature refrigerant flowing through the pipe between the compressor and condenser, the heat loss can be characterized as

$$m_r C_{pr}\left(T_{cp,o} - T_{cd,i}\right) = f\left(\left(\frac{T_{cp,o} + T_{cd,i}}{2}\right) - T_a, m_r\right). \tag{27}$$

In this case, the equation can be expressed from the experiments as

$$m_r C_{pr}\left(T_{cp,o} - T_{cd,i}\right) = \left[\begin{array}{l} \left(1.607 m_r^2 - 0.0298 m_r - 0.0146\right)\left(\left(\frac{T_{cp,o} + T_{cd,i}}{2}\right) - T_a\right) \\ + \left(-20.432 m_r^2 + 1.9399 m_r - 0.293\right) \end{array}\right]. \tag{28}$$

4. SYSTEM SIMULATION

With the mathematical modeling of each main component in the system, the simulation is created to determine the energy consumption of the system at various possible combinations of the conventional chilled water system and the ice thermal energy storage (ITES) system. The computational steps are shown in Fig. 11.

As shown in Fig.11, the simulation consists of two parts, chilled water system and ITES system. The input parameters of the simulation are the total cooling load, Q_{load}; the compressor speed of the ITES system, N_{dc}; the mass flow rate of refrigerant for the ITES system, $m_{r,dc}$; the initial temperature of water in the storage tank, T_{wi}; the ambient temperature, T_{amb} and the properties of the system working fluid.

The cooling load is divided into two parts for chilled water system and ITES system, $Q_{load,ac}$ *and* $Q_{load,dc}$. For the chilled water system, the trial and error has been done to find out the suitable mass flow rate of the refrigerant at the given cooling load. Moreover, the power input of the compressor, the heat transfer rates at the condenser and the chiller are also the output values of the program.

For the ice storage part, the calculation is under the assumption that the leaving temperature of the refrigerant of the ice storage tank is equal to the temperature of the water in the tank because of high turbulence due to the refrigerant injection into the water tank. When the temperature of water is higher than 0.01°C, the calculation is in sensible heat mode. As the water temperature is lower than 0.01°C, the latent heat mode is applied. The outputs of this part are the power consumption at the compressor, the heat transfer rate of the direct contact evaporator and the time consumed for producing ice.

5. RESULTS

5.1 Chilled Water System

In the chilled water system part of the simulation program, after input the initial values of the variables, the compressor work and the heat transfer rate at the chiller are evaluated. The results from the simulation are compared to those of the experiments. The results are illustrated in Figs. 12-13. From the results, it could be found that the compressor work and the heat transfer rate depend on the refrigerant mass flow rate. As the refrigerant mass flow rate increases, these values are also increased. Moreover, it is noted that the values from the simulation program are closed to the experimental results.

5.2 Ice Storage System

For the ice storage simulation, the compressor work, the heat transfer rate at the direct contact evaporator and the time used to produce ice are evaluated. The results are shown in Figs. 14-15 and Table 1. They agree well with those of the experiments.

As shown in Figs. 14-15, the refrigerant mass flow rate has an effect on the both of the compressor work and the heat transfer rate at the direct contact evaporator. As the mass flow rate increases, the compressor work and the heat transfer rate are also increased.

The calculation above lead to the determination of the ice mass produced in the ice storage system and the results are shown in Table 1 in which good agreement is seen between the results from the simulation and the experiments.

5.3 Appropriate Sizing of the Ice Storage

In this research work, an office having 18 kW of cooling requirement is considered as a case study. Eight different air conditioning system combinations have been investigated to determine the appropriate possible combinations which relates to the electricity tariff (TOU rate) as shown in Table 2 [10].

The eight categories are as the following:

Category 1. Conventional design (no ice storage). The entire cooling requirement is supported by the chiller unit operating during the occupancy period.

Categories 2-8. Partial storage design. The chiller unit is responsible for the less cooling requirement compared to the conventional system. The cooling load is divided into two parts. The first part is supported by the chiller unit during the occupancy time and the other is supported by the ice produced in the ice storage or ITES system operating during the nighttime. The ratio of the cooling load supported by the chiller unit (kW) to the cooling load supported by the ITES system (kW) for categories 2-8 are 16:2, 14:4, 12:6, 10:8, 8:10, 6:12 and 4:14, respectively.

From the system simulation, the peak energy demand (kW) of each category is shown in Table 3 while the energy consumption (kW-h/day) and the operating cost of each categories are illustrated in Figs. 16-17.

From Table 3, it could be found that the peak energy demand during the on-peak period decreases when the capacity of the ITES system increases. This is due to the fact that the load of the compressor in the chilled water system is shifted to the ITES compressor running during the off-peak period. However, for categories 7 and 8 in which the capacities of the ITES are 12 and 14 kW, respectively, the required period for generating ice is more than 11 hrs. Then the

compressor load of the ice storage overlaps to that of the chilled water system in the on-peak period.

Fig. 16 shows the electrical energy consumption of the system in each category. Similar to Table 3, as the size of the storage increases, the energy consumption of the chiller decreases and that of the storage increases. For categories 2 –5, the total energy consumption does not exceed the conventional system (1st category). For categories 6 – 8, it could be found that the designs are not appropriat since the energy consumption is higher than that of the conventional unit.

To determine the operating cost, it could be seen that the appropriate design is the 5th category whereas the cheapest cost is obtained as shown in Fig. 17. At this condition, the energy demand and energy consumption from the daytime could be shifted to the nighttime when the tariff is lowest. The peak energy demand from 9.7 kW in case of the conventional unit could be reduced to 5 kW (48.7% decreased). The operating cost is reduced from 4,200 baht/month for conventional system to 3,100 baht/month resulting in 27% reduction.

It could be found that this system yields a realistic payback. In this research work, the installation cost of the ice storage system is approximately 70,000 baht and the operating cost is reduced for 1,100 baht/month. If the ITES is chosen to operate during March to October which has high opportunity to use the ice storage system, then, the payback period could be approximately 8 years.

6 CONCLUSION

The mathematical of each main component in the ice thermal energy storage with direct contact evaporator is created and the system simulation to find out the suitable refrigerant mass flow rate at any given cooling load, the time used to produce the required amount of the ice and energy consumption has been carried out with good agreement to the experimental results. It is also indicated that for the office having 18 kW of cooling requirement considered as a case study, the appropriate size of the ITES system is 8 kW. Under this operating condition, the peak electricity demand and the operating cost could be decreased 48.7 % and 27%, respectively comparing to the conventional chiller system. The payback is about 8 years.

Acknowledgement - The authors gratefully acknowledge the support provided by Thailand Research Fund and The Joint Graduate School of Energy and Environment for carrying out this study.

REFERENCES

1. S.A. Tassou and Y.K. Leung, Energy Conservation in Commercial Air Conditioning through Ice Storage and Cold Air Distribution Design, *Heat Recovery Systems & CHP*, Vol.12, pp.419-425, 1992.
2. Simmonds P., A Control Strategy for Chilled Water Production, *ASHRAE Journal*, pp. 30-36, January 1994.
3. Limmeechokchai, B. and Chungpaibulpatana, S., Application of Cool Storage Air Conditioning in Commercial Building Sector, Paper accepted for publication in *Applied Energy*, September 2000.
4. Crane, J. and Dunlop, C., Ice Storage System for a Department Store, *ASHRAE Journal*, pp. 49-52, January 1994.
5. Guluska, E., Thermal Storage System Reduces Costs of Manufacturing Facility, *ASHRAE Journal*, pp. 50-52, March 1994.
6. Subbaiyer, S., Andhole, T.M. and Helmer, W.A., Computer Simulation of a Vapor-Compression Ice Generator with a Direct Contact Evaporator, *ASHRAE Transactions*, part 1, pp. 118-126, paper number 3448, 1991.
7. Kiatsiriroat, T., Siriplubpla, P. and Nuntaphan, A., Performance Analysis of a Refrigeration Cycle Using a Direct Contact Evaporator, *International Journal of Energy Research*, **22**, 1179-1190, 1998.
8. Kiatsiriroat, T., Chowcheun, K. and Wibulswas, P., Simulation of a Standard Vapor-Compression Refrigeration System, *ASEAN Journal on Science & Technology for Development*, Vol 11, no.1, pp. 167-180, 1994.
9. Stoecker, W.F., *Design of Thermal Systems*, McGraw-Hill, USA, 1989.

10. Electricity Generating Authority of Thailand (EGAT), 1997. *Thailand power development plan PDP 1997-01.* System Planning Department. Bangkok, Thailand.

NOMENCLATURE

C_P	specific heat capacity (kJ/kgK)
DC	demand charge (Baht/kW)
EC	energy charge (Baht/unit)
h	specific enthalpy (kJ/kg)
k	polytropic index
L	latent heat (kJ/kgK)
m	mass flow rate (kg/s)
M	mass (kg)
N	compressor speed (rps)
OC	overall charge (Baht))
P	pressure (MPa)
Q	heat transfer rate (kW)
T	Temperature (°C)
Δt	period of time (s)
UA	overall heat transfer coefficient (kW/m^2K)

Subscripts

a	air
cd	condenser

ch chiller

cp compressor

ev evaporator

ex expansion valve

i inlet

o outlet

r refrigerant

w water

CAPTIONS OF FIGURES AND TABLES

Fig. 1. Schematic diagram of the experimental set-up.

Fig. 2. The relation between pressure ratio of the compressor and a function of $m_r T_{cp,i}^{0.5}/P_{cp,i}$.

Fig. 3. The relation between pressure ratio of the compressor and a function of $m_r T_{cp,o}^{0.5}/P_{cp,o}$.

Fig. 4. The relation between mass flow rate of the refrigerant and the polytropic index of the compressor in chilled water system.

Fig. 5. The relation between the pressure ratio in the chilled water system and the refrigerant mass flow rate.

Fig. 6. Schematic diagram of the experimental set-up for the ice storage system.

Fig. 7. The relation between pressure ratio of the compressor in the ice storage system and a function of $m_r T_{cp,o}^{0.5}/P_{cp,o}$ and N.

Fig. 8. The relation between mass flow rate of refrigerant and the polytropic index of the compressor in ice storage system.

Fig. 9. The effect of mass flow rate of air and total heat transfer coefficient to outlet temperature of air.

Fig. 10. The relation between pressure ratio of the expansion valve in the ice storage system and mass flow rate of refrigerant at various compressor speeds.

Fig. 11. Information flow diagram of the system simulation.

Fig. 12. Compressor work of the chilled water system at various refrigerant mass flow rates.

Fig. 13. The chiller cooling load at various refrigerant mass flow rates.

Fig. 14. Compressor work of the ice storage system at various refrigerant mass flow rates.

Fig. 15. The direct contact evaporator cooling load at various refrigerant mass flow rates.

Fig. 16. Energy consumed in each category.

Fig. 17. Operating cost in each category.

Table 1. The comparison of ice formation between the simulation and the experiment.

Table 2. Electricity cost (TOU Rate) for commercial building.

Table 3. The peak energy demand occurred during on-peak period at various categories.

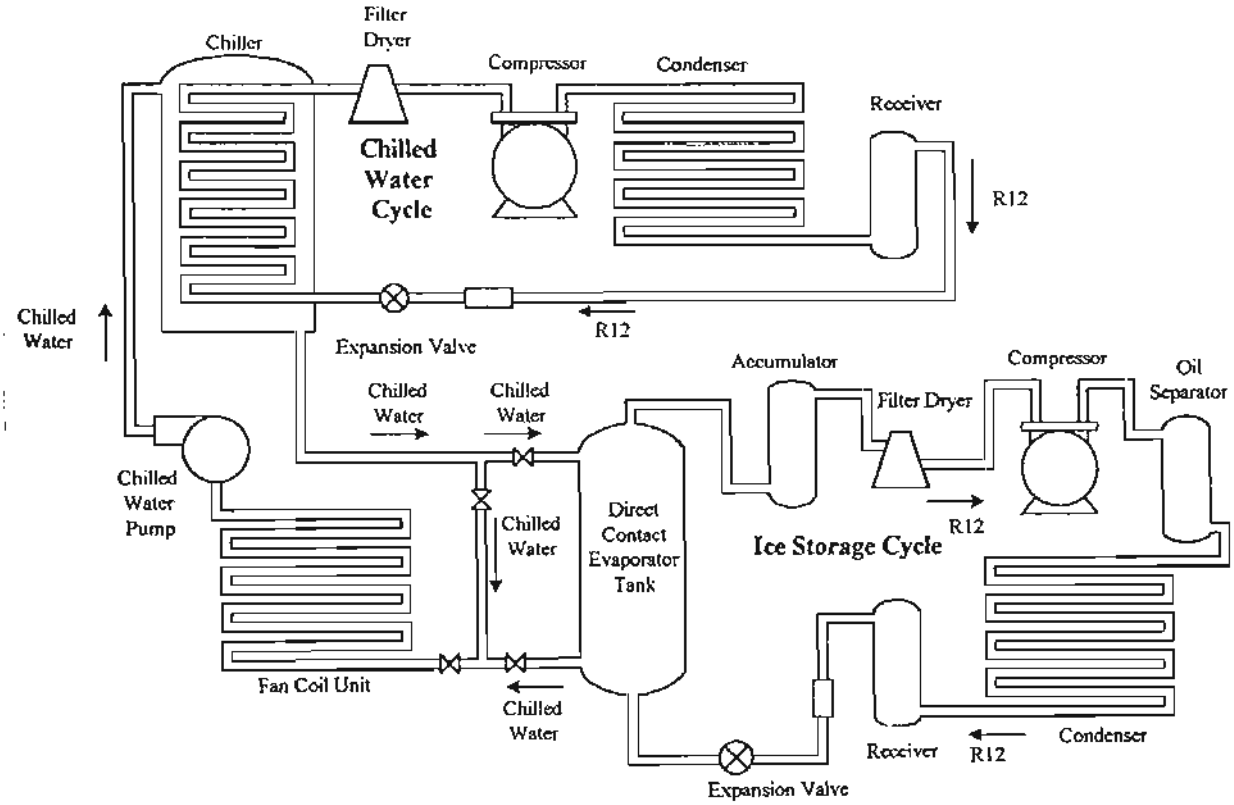

Fig.1. Schematic diagram of the experimental set-up.

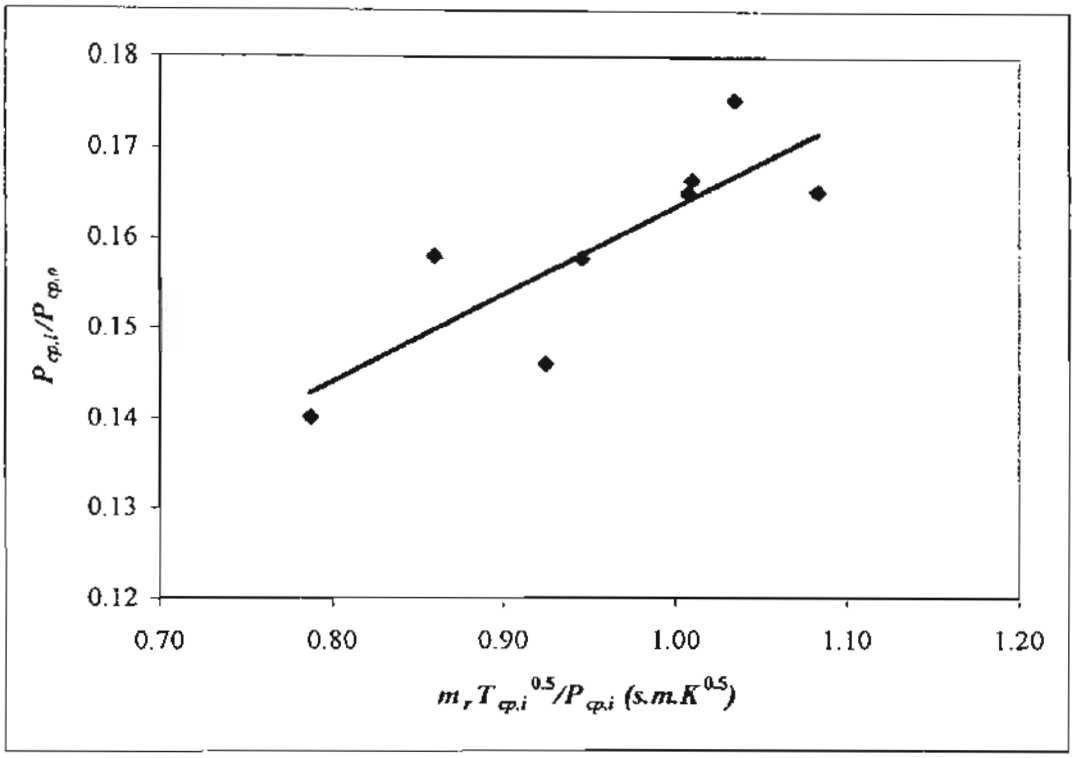

Fig.2. The relation between pressure ratio of the compressor and a function of $m_r T_{cp,i}^{0.5}/P_{cp,i}$.

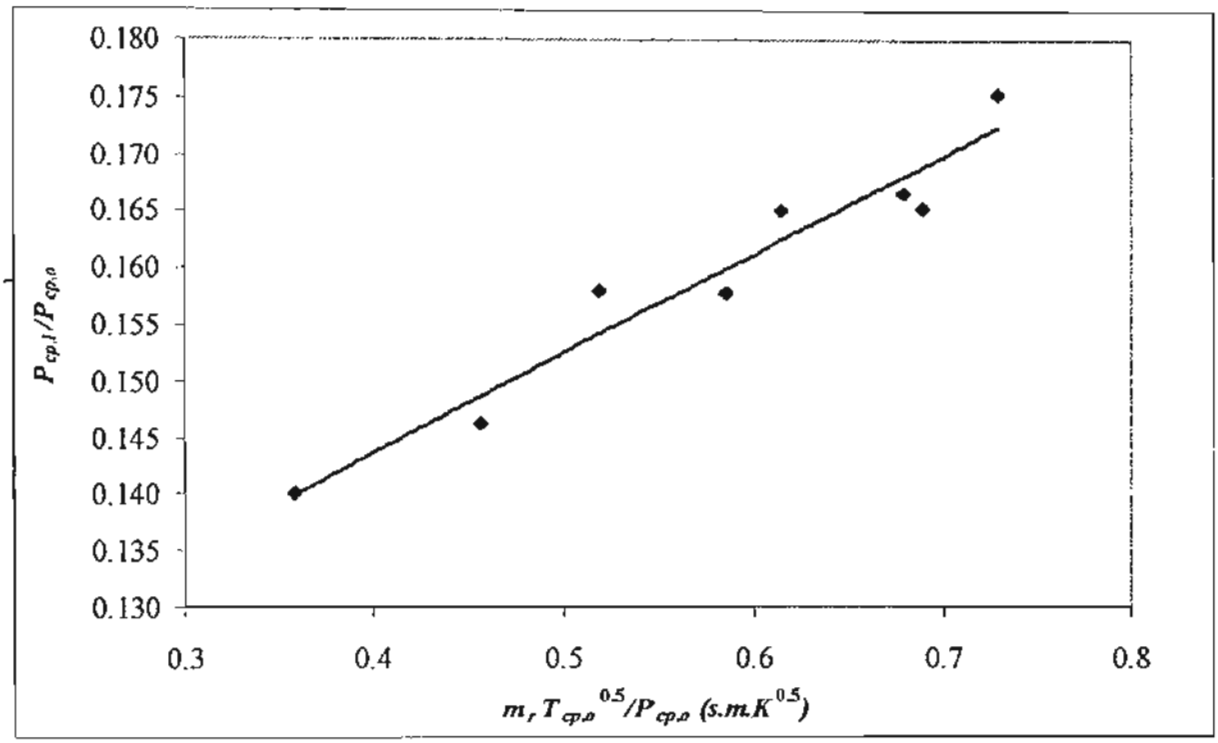

Fig.3. The relation between pressure ratio of the compressor and a function of $m_r T_{cp,o}^{0.5}/P_{cp,o}$

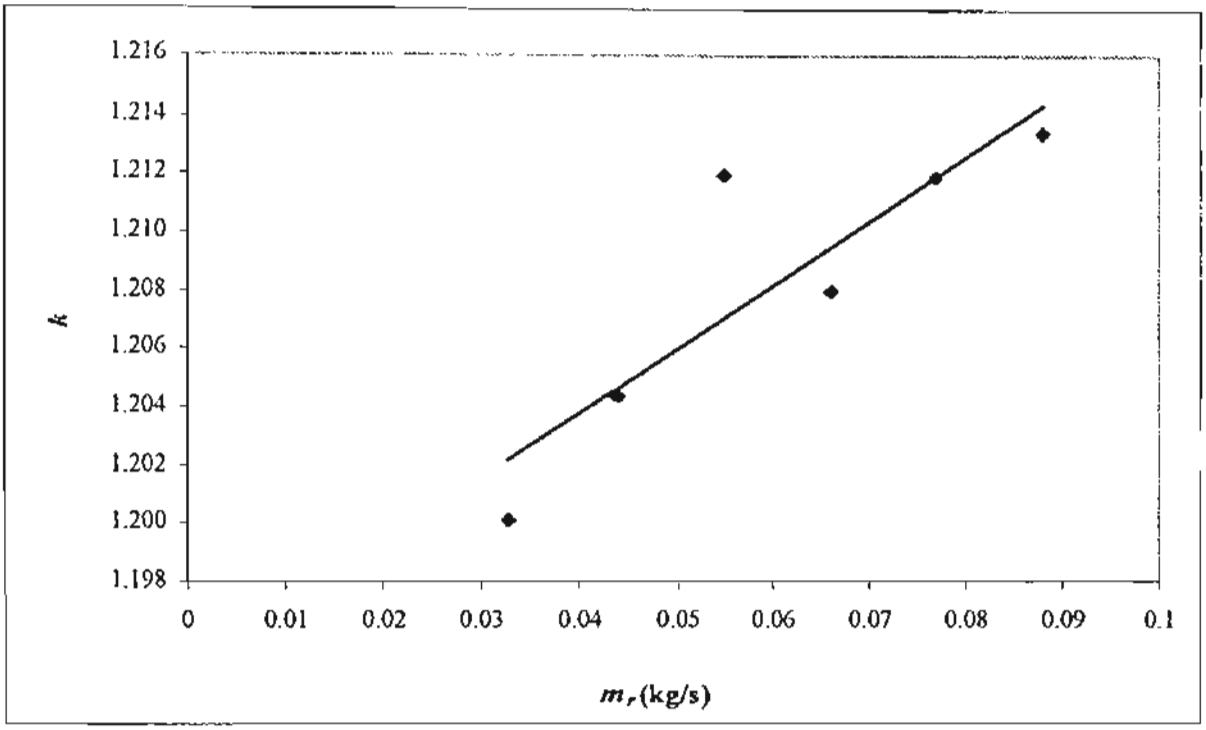

Fig.4. The relation between mass flow rate of the refrigerant and the polytropic index of the compressor in chilled water system.

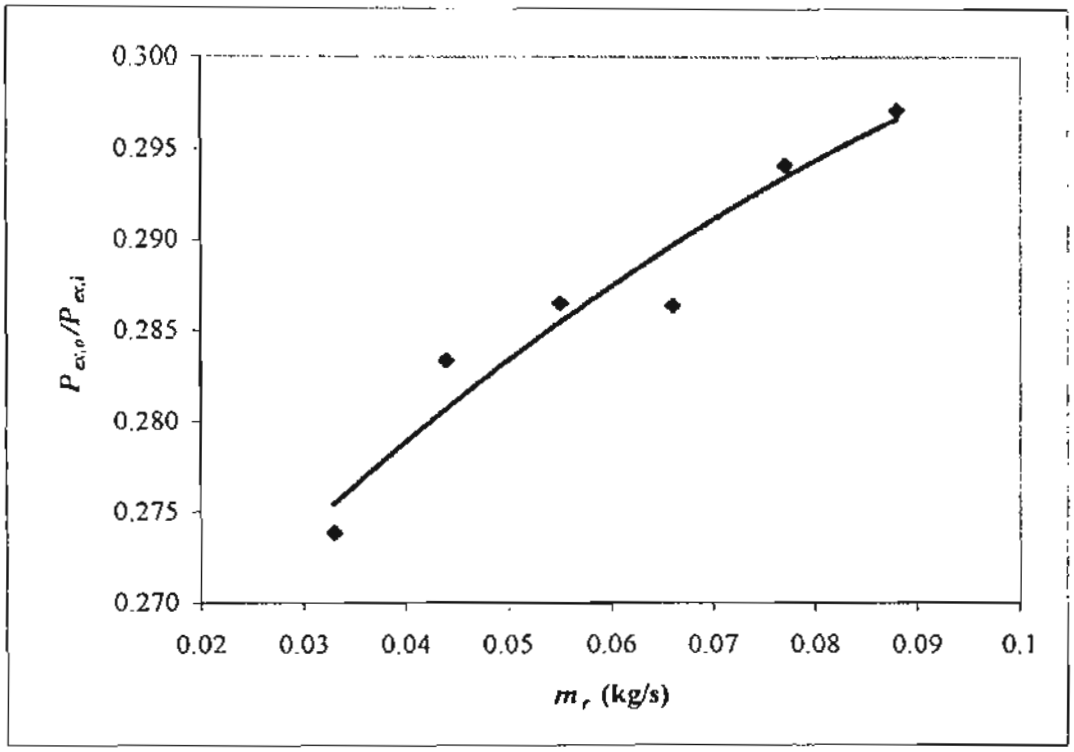

Fig.5. The relation between the pressure ratio in the chilled water system and the refrigerant mass flow rate.

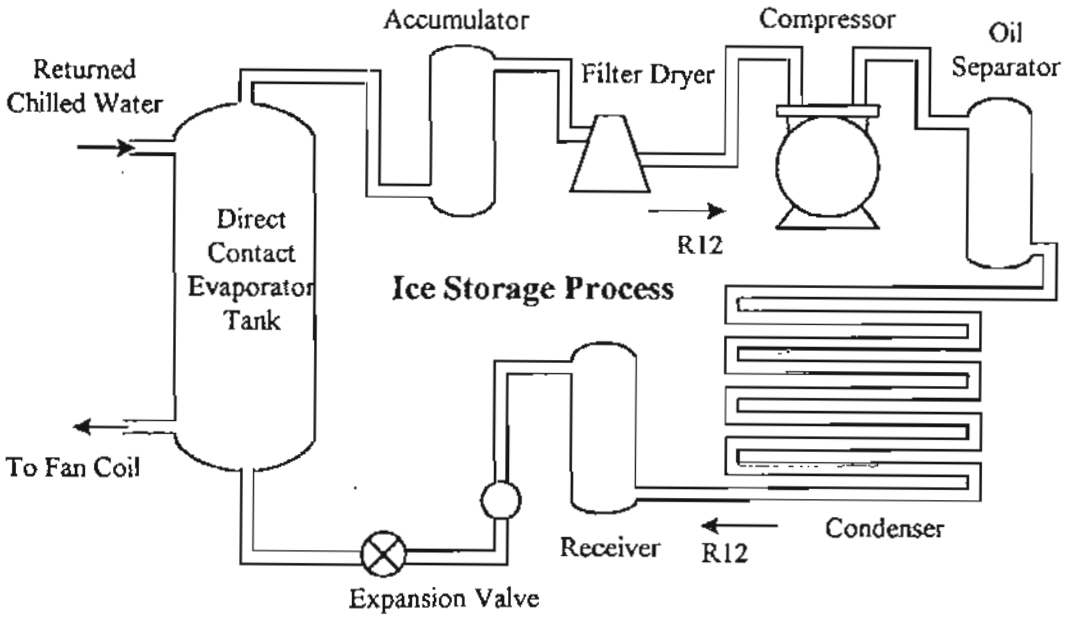

Fig.6. Schematic diagram of the experimental set-up for the ice storage system.

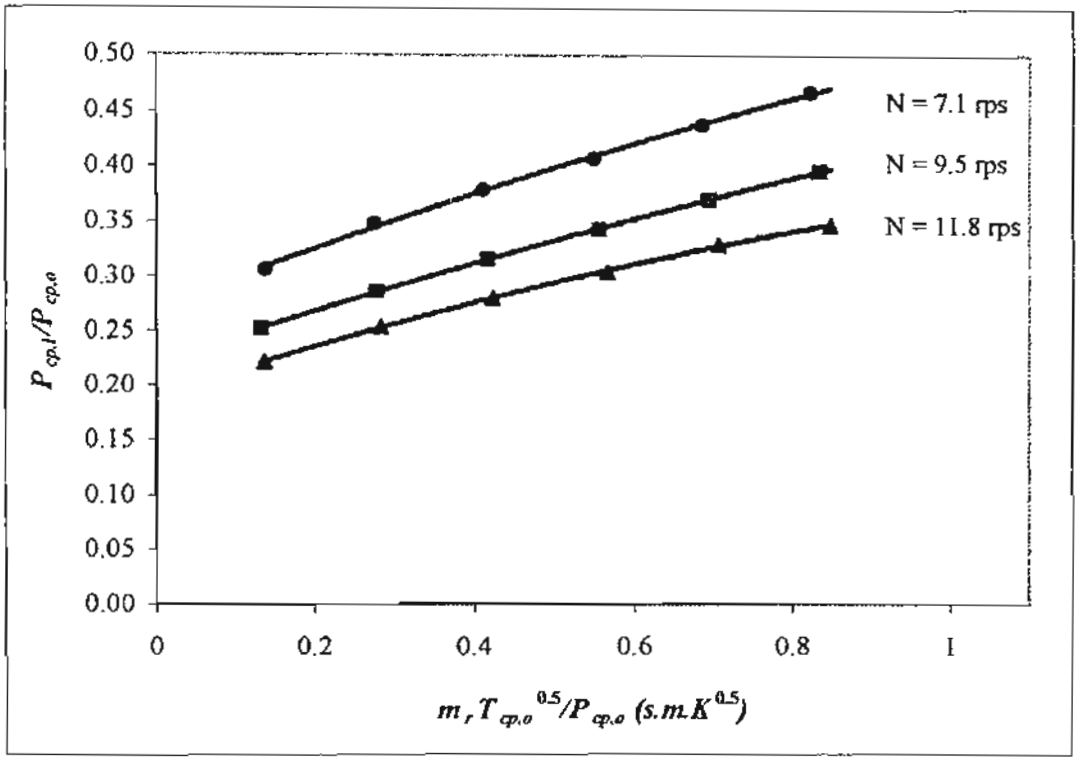

Fig.7. The relation between pressure ratio of the compressor in the ice storage system and a function of $m_r T_{cp,o}^{0.5}/P_{cp,o}$ and N.

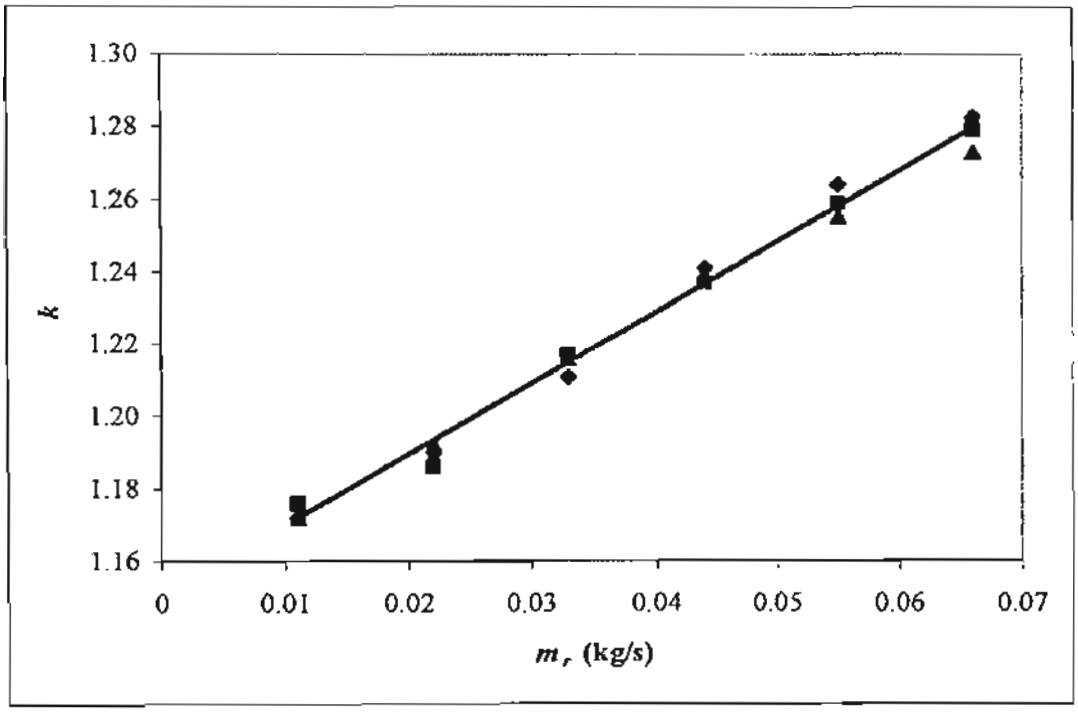

Fig.8. The relation between mass flow rate of refrigerant and the polytropic index of the compressor in ice storage system.

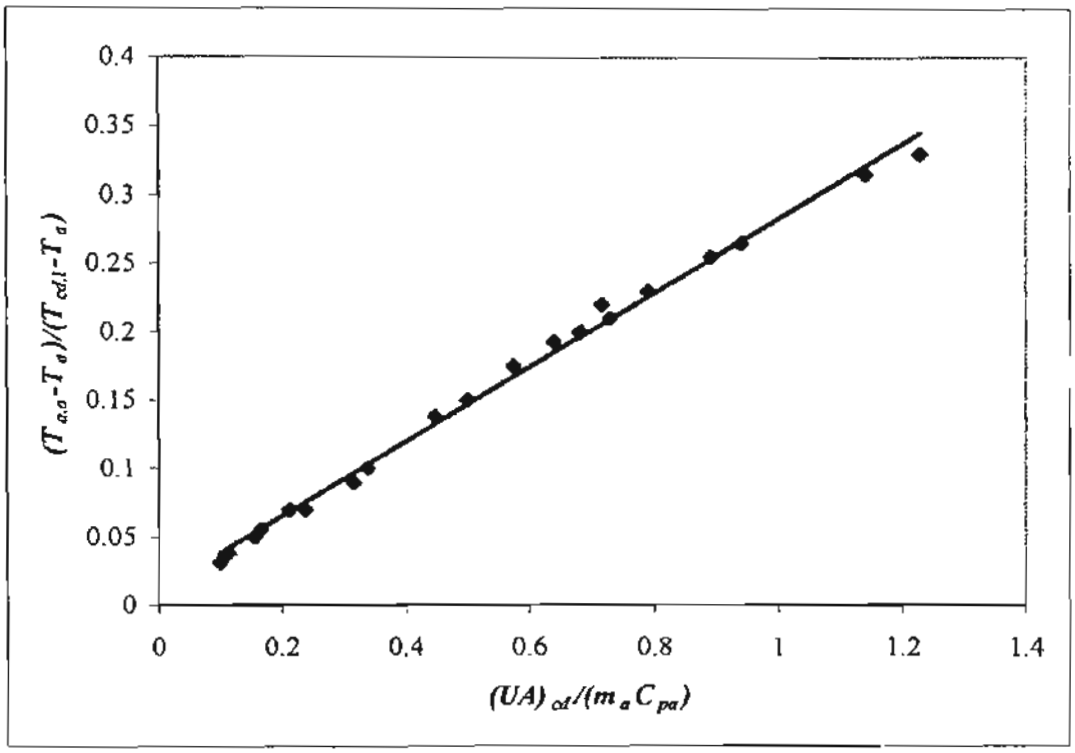

Fig.9. The effect of mass flow rate of air and total heat transfer coefficient to outlet temperature of air.

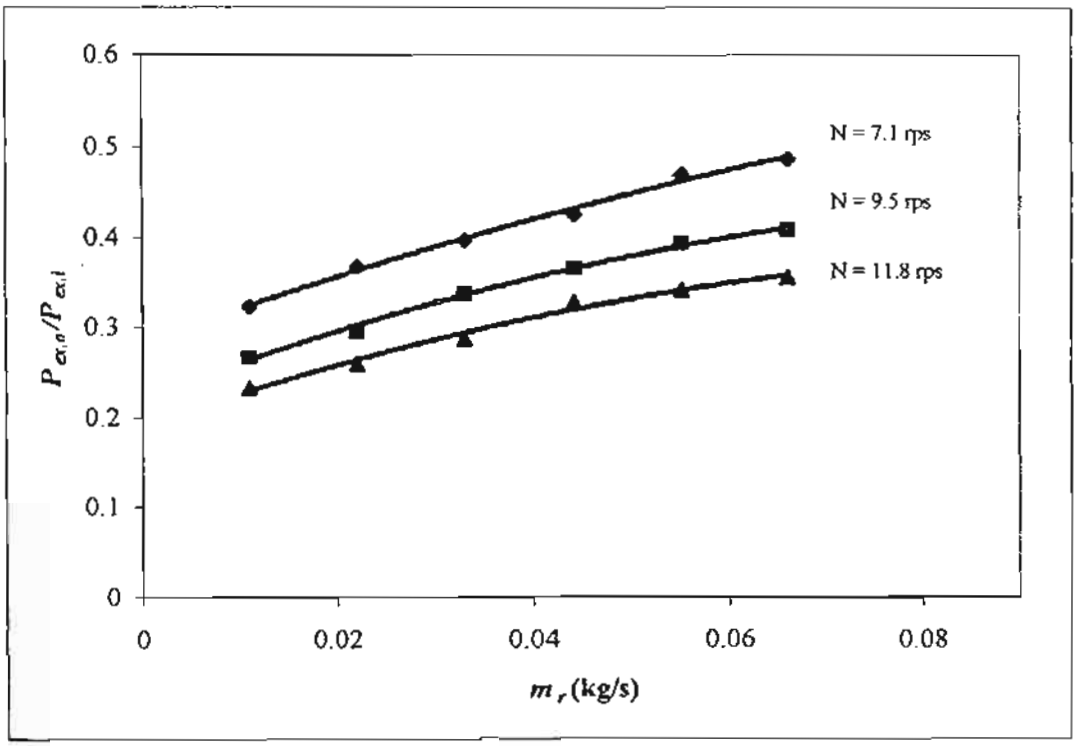

Fig.10. The relation between pressure ratio of the expansion valve in the ice storage system and mass flow rate of refrigerant at various compressor speeds.

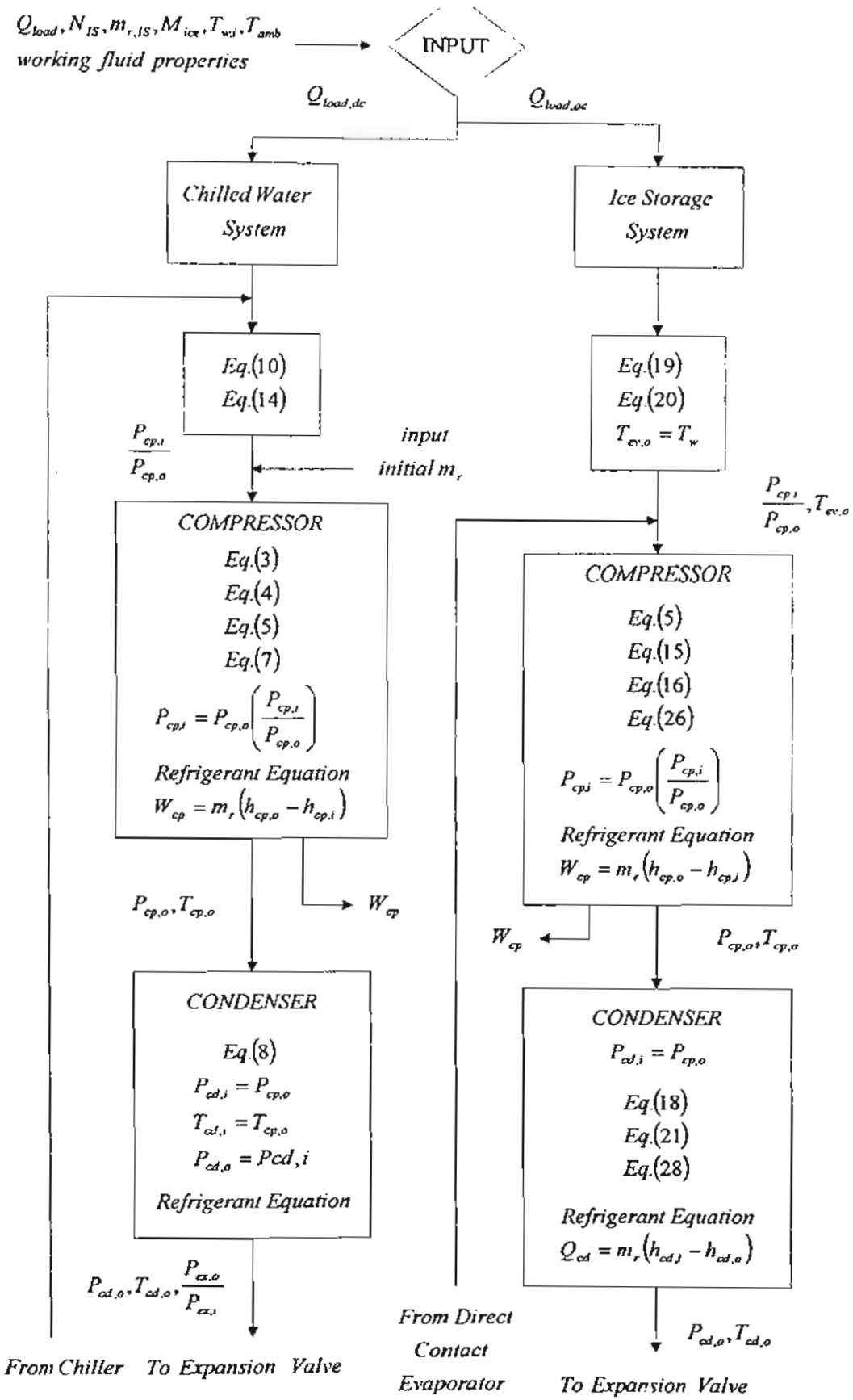

Fig. 11. Information flow diagram of the system simulation.

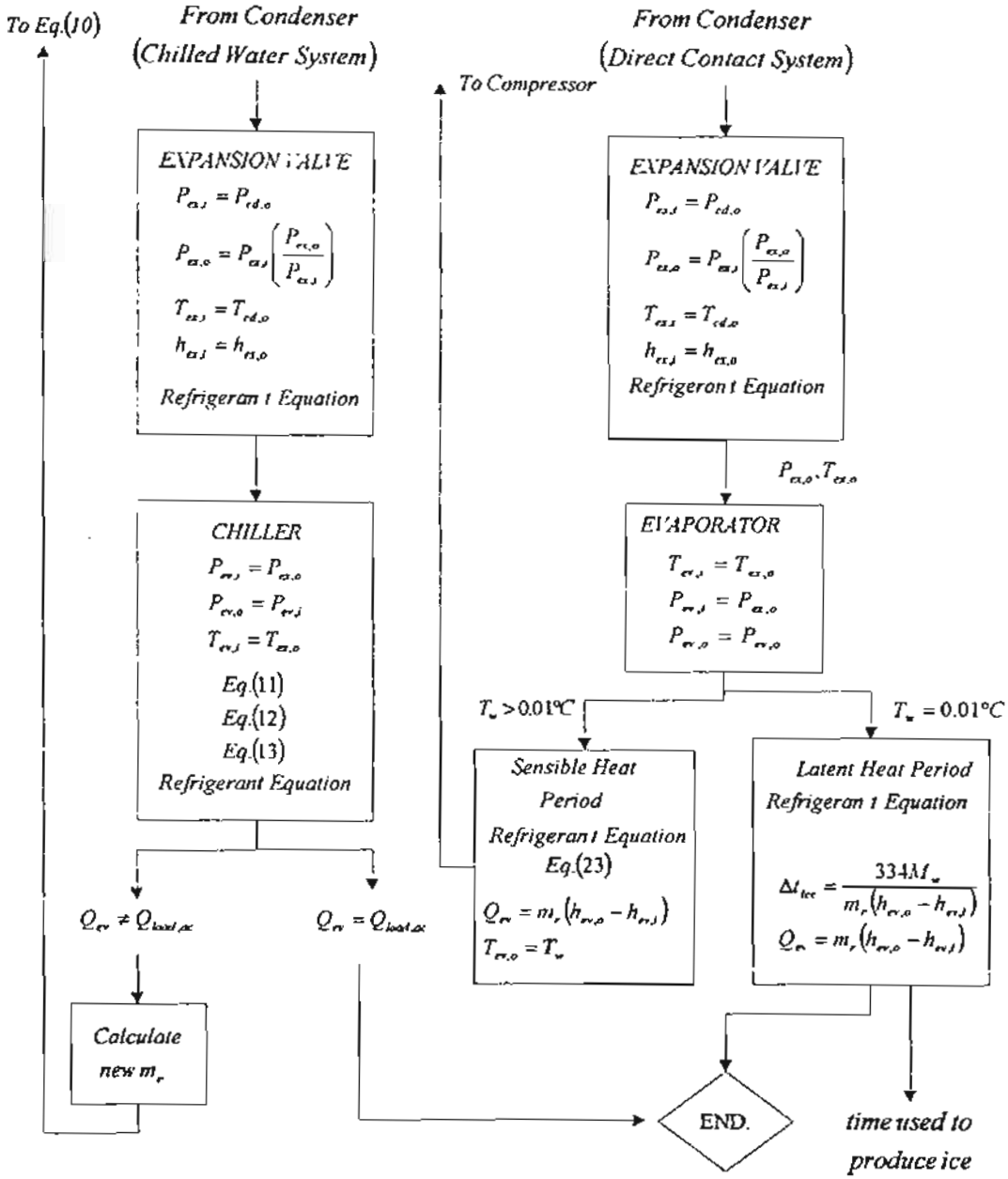

Fig. 11. Information flow diagram of the system simulation (continued).

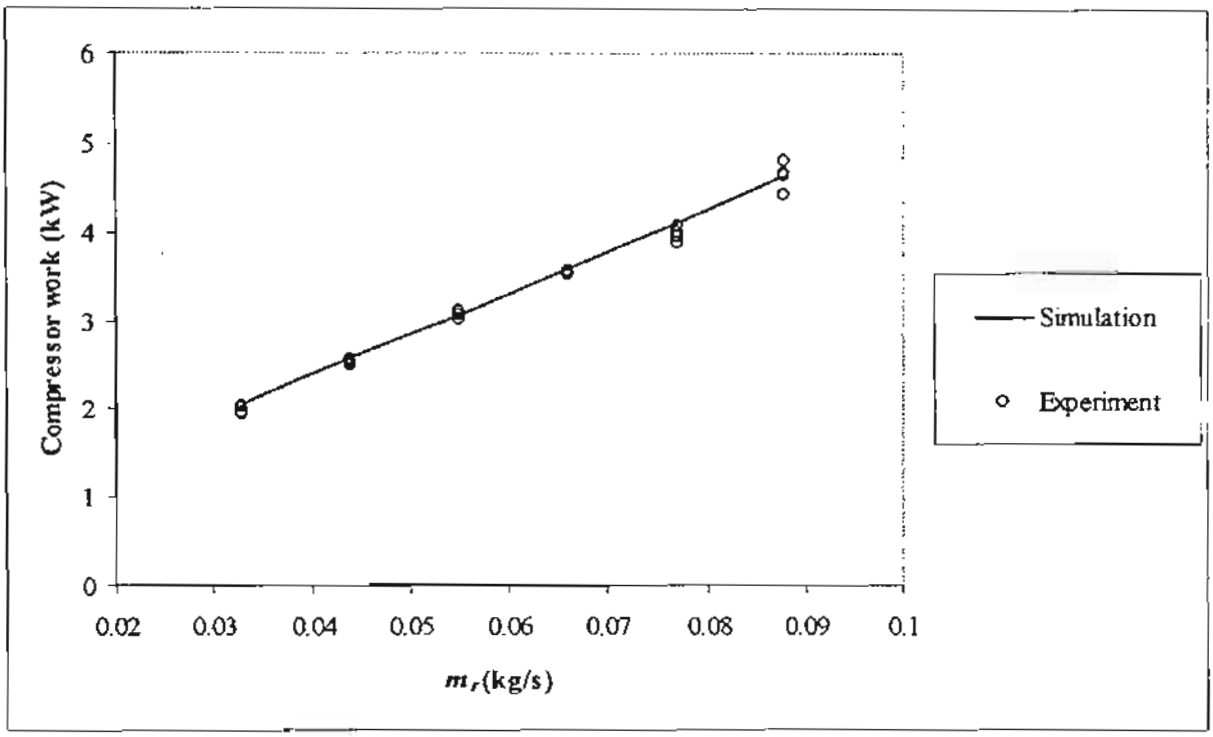

Fig. 12. Compressor work of the chilled water system at various refrigerant mass flow rates.

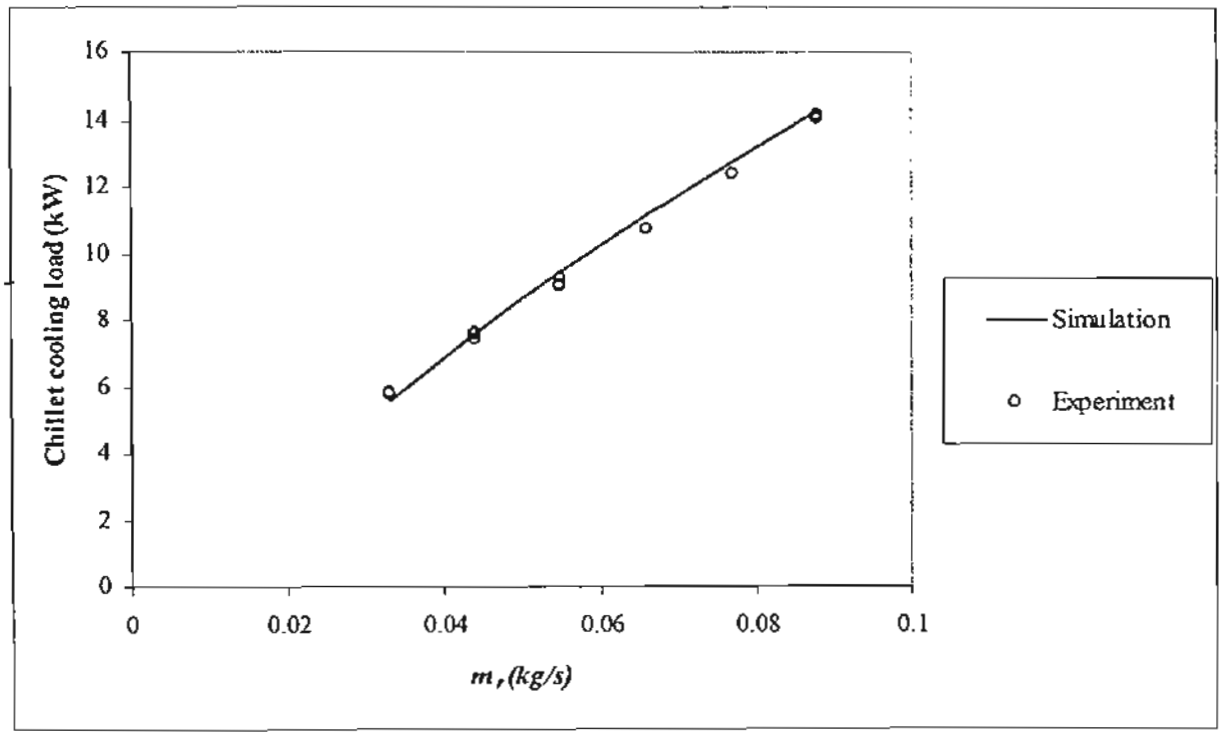

Fig. 13. The chiller cooling load at various refrigerant mass flow rates.

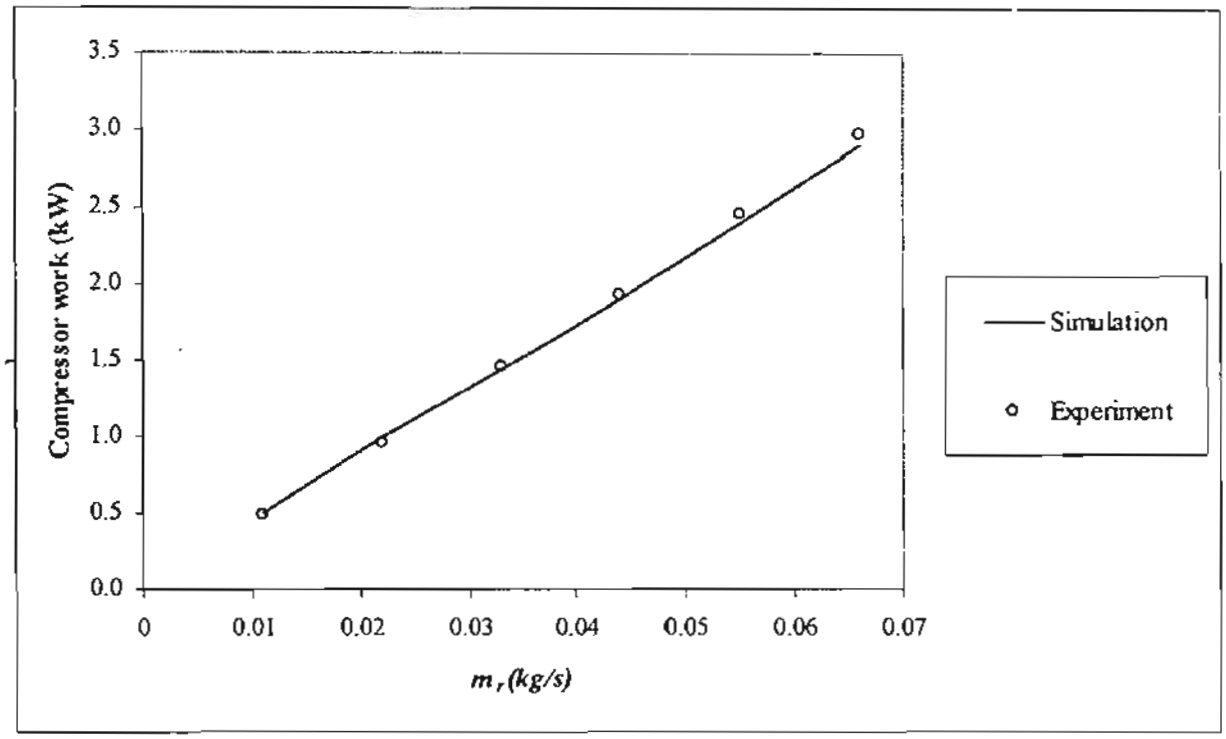

Fig. 14. Compressor work of the ice storage system at various refrigerant mass flow rates.

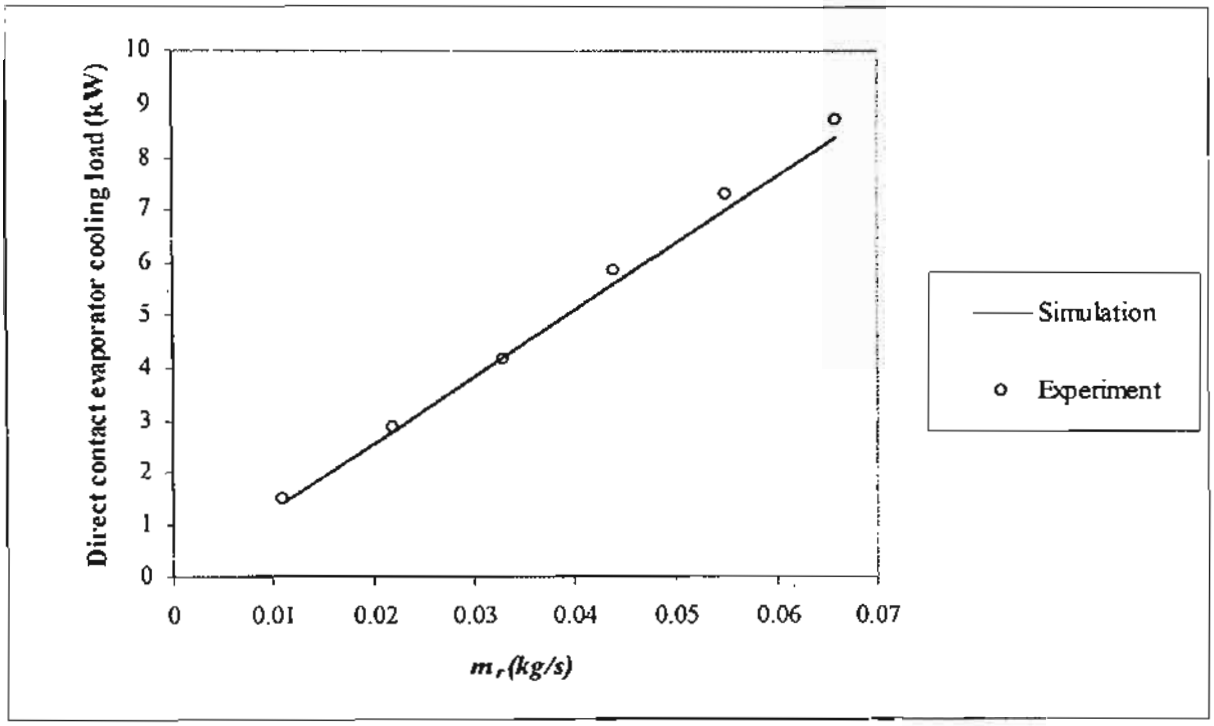

Fig. 15. The direct contact evaporator cooling load at various refrigerant mass flow rates.

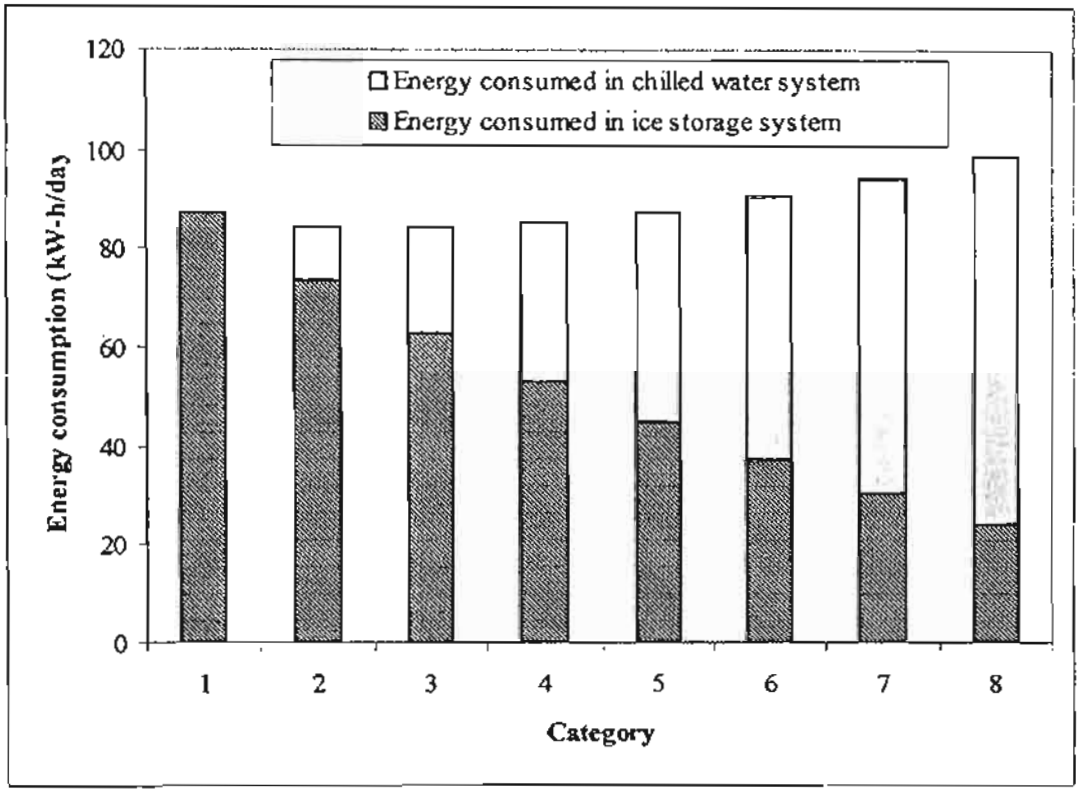

Fig.16. Energy consumed in each category.

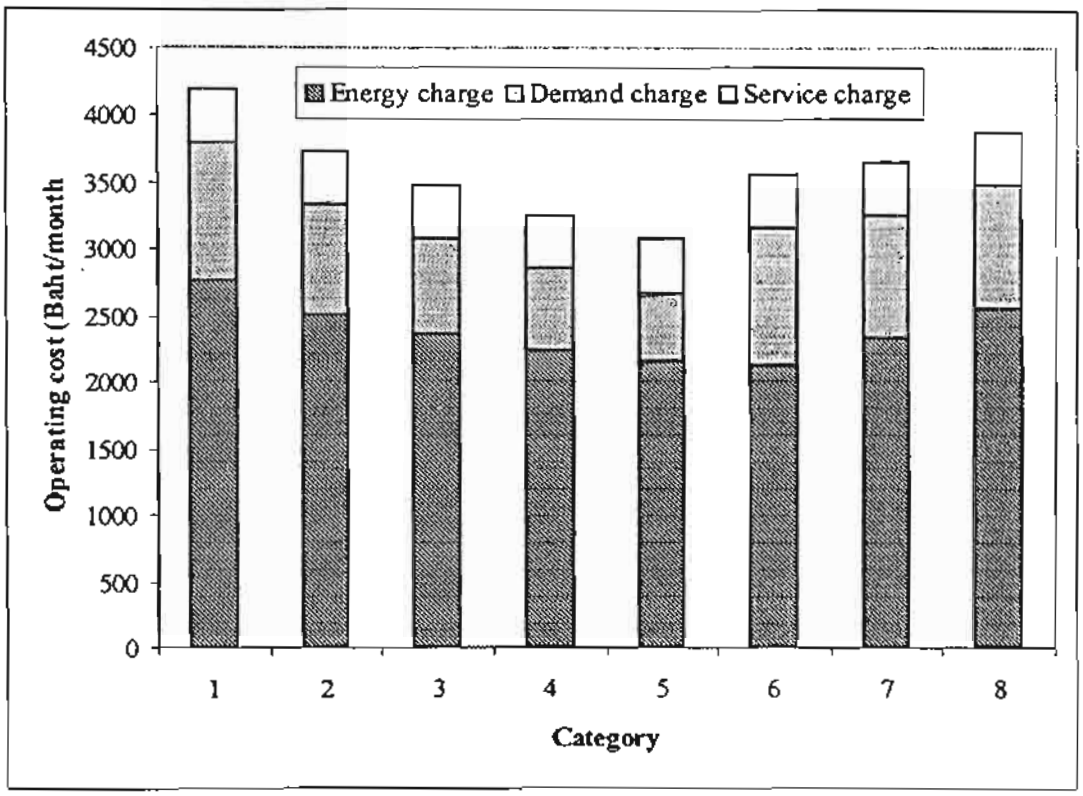

Fig. 17. Operating cost in each category

Table 1. The comparison of ice formation between the simulation and the experiment.

Mass of water in storage tank (kg)	m_r (kg/s)	N (rps)	Initial water temp. (°C)	Tamb (°C)	Produced ice mass (kg) (sim.)	Time (hr) (sim.)	Produced ice mass (kg) (exp.)	Time (hr) (exp.)
250	0.077	11.8	18.0	29.2	250	3.66	212	3.59
250	0.100	11.8	16.5	30.2	250	3.11	209	3.23
300	0.066	11.8	15.0	28.5	300	5.01	272	4.98
300	0.100	11.8	15.4	26.8	300	3.67	269	3.62

Table 2. Electricity cost (TOU Rate) for commercial building [10]

Voltage	Demand Charge (Baht/kW)	Energy Carge (Baht/unit)			Service charge (Baht/month)
	1*	1*	2*	3*	
>115 kV	102.80	1.5349	0.6671	0.6062	400.00
69 kV	158.88	1.6292	0.6769	0.6153	400.00
22 –23 kV	200.93	1.7736	0.6861	0.6236	850.00
<22 kV	214.95	1.8891	0.7283	0.6616	850.00

1* Monday – Saturday 09.00 – 22.00 (On-peak)

2* Monday – Saturday 22.00 – 09.00 (Off-peak)

3* Sunday 00.00 – 24.00 (Off-peak)

Table 3. The peak energy demand occurred during on-peak period at various categories.

Category	Ice storage system capacity (kW)	Peak energy demand		
		Chilled water system (kW)	Ice storage system (kW)	Total (kW)
1	0	9.7	-	9.7
2	2	8.2	-	8.2
3	4	7.0	-	7.0
4	6	5.9	-	5.9
5	8	5.0	-	5.0
6	10	4.1	-	4.1
7	12	3.4	5.5	8.9
8	14	2.6	5.5	8.1

Heat Transfer Model of a Direct Contact Evaporator

T. Kiatsiriroat, S. Vithayasai and N. Vorayos
Department of Mechanical Engineering
Chiang Mai University, Chiang Mai 50200, Thailand

A. Nuntaphan
South East Asia Center for Training in Energy for Development
Electricity Generating Authority of Thailand
Mae Moh, Lampang 52220, Thailand

N. Vorayos
Joint Graduate School of Energy and Environment
King Mongkut's University of Technology Thonburi
Bangkok 10140, Thailand

ABSTRACT

This research work studies heat transfer characteristic of a direct contact evaporator. A cold two-phase refrigerant (R12 or R22) is injected into water kept in a storage tank to exchange heat with the water directly. The water temperature is reduced to the freezing point and ice could be formed. The lump model is used to predict the water temperature and it is found that this model can predict the water temperature quite well. A correlation which relates the dimensionless parameters such as Stanton number, Stephan number, Prandtl number and pressure ratio is also developed.

Keywords: *Direct contact heat exchange, Ice thermal energy storage, Heat transfer correlation.*

Submitted to **Applied Energy, June, 2001**

Address of Correspondence and Proof:
Prof. Dr. Tanongkiat Kiatsiriroat
Department of Mechanical Engineering, Faculty of Engineering,
Chiang Mai University, Chiang Mai 50200, Thailand.
Tel:6653-944144 Fax:6653-944145
E-mail: *tanong@dome.eng.cmu.ac.th*

INTRODUCTION

For several years, the electrical energy consumption has increased and becomes a serious problem in developing countries. In Thailand, the electricity demand increases approximately 12% every year [1]. The demand-side management policy is set as a method to overcome this problem by charging the consumers with a high premium rate for the energy consumed during the peak period and a low rate during the off-peak period. Uniform load factor and reduction of peak demand then are anticipated.

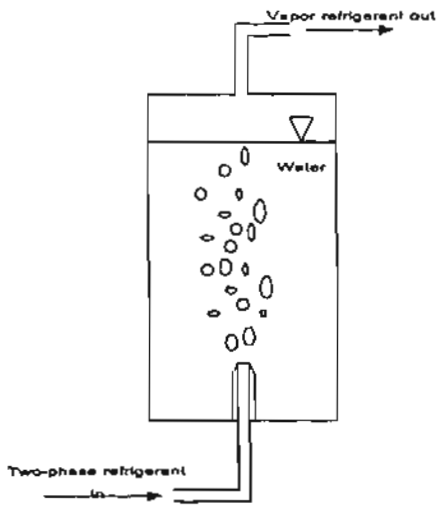

Figure 1 Direct contact evaporator.

In case of commercial building, 60% of the electrical energy consumption comes from the air-conditioning system [2]. This system is normally operated during the daytime or on-peak period which consequently increases the electrical peak demand and thereby is charged with a high electrical charge rate. To alleviate this problem, ice thermal energy storage has been conducted. During the nighttime or off-peak period, ice could be formed in a storage tank and

during the daytime a circulation of cool water from a storage tank is used for air-conditioning purpose. As the result, the uniform load and reduction of the peak demand are achieved.

The most common design of ice thermal energy storage is ice-on-coil system. The refrigerant is circulated inside the submerge coil in a water tank on which ice formation takes place. However, because of low thermal conductivity of ice, the ice layer forming on the coil severely inhibits the transfer of heat. To improve the performance of the ice storage, the direct contact evaporator is conducted. Figure 1 shows the principle of the direct contact evaporator. The cold two-phase refrigerant is injected into the water in the storage tank to extract heat from water directly. The water temperature is decreased and ice is formed when the freezing point is reached. The refrigerant vapor leaves the storage tank through the upper channel.

Some studies on the injection of immiscible fluid into phase change materials for exchangining heat directly have been carried out. The applications are thermal storages for heating and a few for cooling purposes. Blair et al. [3] studied the heat transfer characteristic of R113 droplet injected into a water column. It was found that the column height affected the degree superheat of the refrigerant and the mass flow rate of refrigerant played an important role on the volumetric heat transfer coefficient which approximately equaled 122 kW/m^3K. Sideman and Gat [4] also found that the volumetric heat transfer coefficient of pentane injecting into water was about180 kW/m^3K which was in the same order as Blair et al. In contrast, Goodwin et al. [5] reported that the volumetric heat transfer coefficient of pentane injecting into water was only about 3-8 kW/m^3K. However no further explanation was elaborated.

Subbaiyer et al. [6] showed a simulated result of a refrigeration unit with a direct contact evaporator. The unit required only 50-60% of electrical energy consumption per ton of refrigerant compared with a cooling coil ice generator. Kiatsiriroat et al. [7] studied the

phenomenon of ice forming around a jet stream of refrigerant injected from the bottom of a water column. Different types of refrigerant, R12, R22 and R134a were used. It was found that the stream of R22 showed better heat transfer, and ice could be formed quicker than those with the other refrigerants. A numerical model to predict the water temperature and the thickness of ice forming was developed, and the results agreed quite well with those of experiment.

In this present study, the heat transfer model of a direct contact evaporator has been investigated. R12 and R22 are selected as the refrigerants and water is chosen as the phase change material. The effects of the volume of water, the inlet temperature and the mass flow rate of refrigerant are investigated and their relation in terms of dimensionless groups is also developed.

THE EXPERIMENTAL SETUP

Figure 2 shows the experimental setup which consists of a direct contact evaporator, a dryer unit, a compressor - condensing unit, a receiver tank and an expansion valve. The direct contact evaporator is a stainless steel storage tank with 30 cm diameter and 110 cm height. The refrigerant from a receiver is injected through the expansion valve to reduce the pressure and temperature. This valve not only controls the mass flow rate of the refrigerant but also controls the temperature and the pressure of refrigerant injected into the storage tank. The cold two-phase refrigerant injected extracts heat from the water directly. As a result, the water temperature is decreased and ice could be formed when the temperature reaches the freezing point. The refrigerant after getting heat becomes vapor and leaves the storage tank to the compressor-condenser unit. The dryer unit is used to eliminate the moisture which might come along with the

refrigerant vapor. The vapor condenses in the condensing unit and the liquid refrigerant returns back to the receiver.

In this study, the refrigerant mass flow rate, the inlet and the outlet temperatures and pressures at the expansion valve, and the water temperature of the storage tank are recorded. Table 1 shows the testing conditions of the experiment.

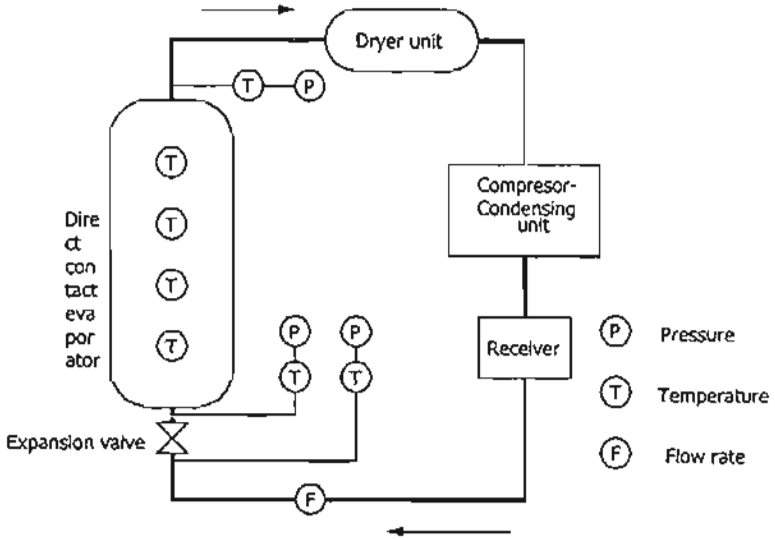

Figure 2 Schematic diagram of the experimental apparatus.

Table 1 The testing conditions of this research work.

Item	Conditions
Mass of water in a storage tank	20-40 kg
Mass flow rate of refrigerant	0.02-0.08 kg/s
Inlet temperature of refrigerant	-8 – -15 °C

MATHEMATICAL MODEL

In our previous studies [2, 8, 9], it was found that high turbulence was found in the water column during the refrigerant injection then the temperature of water was found to be uniform. Moreover, the temperature of the refrigerant that leaving out from the water was close to that of water in the storage tank. Therefore the lumped model could be conducted to analyze the thermal characteristic of the water in the storage tank.

The energy balance at the direct contact evaporator could be written as

$$\frac{d}{dt}(m_w h_w) + m_t Cp_t \frac{dT_w}{dt} = \dot{m}_r (h_{ri} - h_{ro}) + (UA)(T_a - T_w). \qquad [1]$$

The left-hand terms are the rate of enthalpy changes of the water and the container respectively. The first right-hand term is the rate of enthalpy change of the refrigerant and the final term is the external heat gain from the surrounding ambient. When the unit is well insulated, the heat gain could be neglected.

During the sensible heat process and the tank temperature is assumed to be the same as that of the water inside, equation [1] could be rewritten in numerical form as

$$T_w^{t+\Delta t} = T_w^t + \frac{\dot{m}_r (h_{ri} - h_{ro}) \Delta t}{m_t Cp_t + m_w Cp_w} \quad . \qquad [2]$$

During the ice formation, the temperature of water is constant around the freezing point. Consequently, equation [1] could be written as

$$m_w \frac{dh_w}{dt} = \dot{m}_r (h_{ri} - h_{ro}) \Delta t \qquad [3]$$

or

$$h_w^{t+\Delta t} - h_w^t = \frac{\dot{m}_r \Delta t}{m_w}\left(h_{ri} - h_{ro}\right) \quad . \qquad [4]$$

$$m_{ice}^t = \frac{m_w\left(h_l - h_w^t\right)}{\lambda} \qquad [5]$$

With the initial condition and the properties of the refrigerant entering, the temperature decrease during the sensible heat process and the amount of ice formation during the latent heat process could be evaluated.

RESULTS AND DISCUSSION

Thermal Analysis of the Direct Contact Evaporator

Figures 3 and 4 show the water temperature in the storage tank compared with that evaluated from the lump model. Since adiabatic storage tank is assumed the temperature from the model drops slightly quicker than that of the experiment. Figure 3 also shows the effect of the refrigerant mass flow rate on the water temperature in the storage tank. When the mass flow rate increases higher heat transfer rate is obtained which results in quicker drop of the water temperature.

Figure 4 shows the effect of the water volume on the rate of temperature drop. It is found that higher amount of the water results in higher the total heat capacity and the temperature drops with a lower rate.

Figure 5 shows the comparison between the amounts of ice formed in the experiment with those from the model. The model gives higher amount of ice than the experimental results approximately 20-30% because of quicker temperature drop.

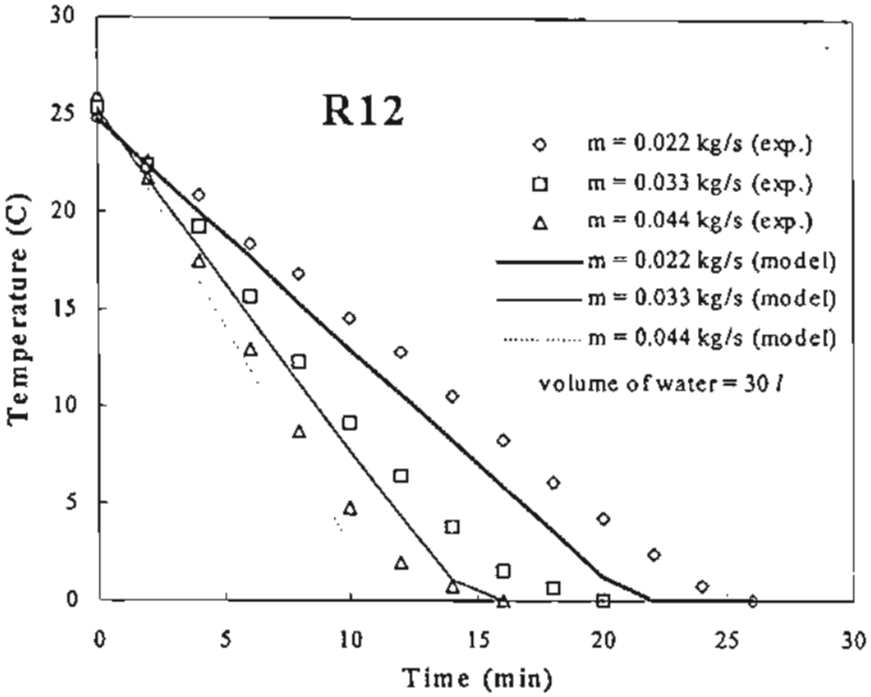

Figure 3 Comparison of water temperatures in the storage tank between the experiment and the lump model at various refrigerant mass flow rates; volume of water = 30 l.

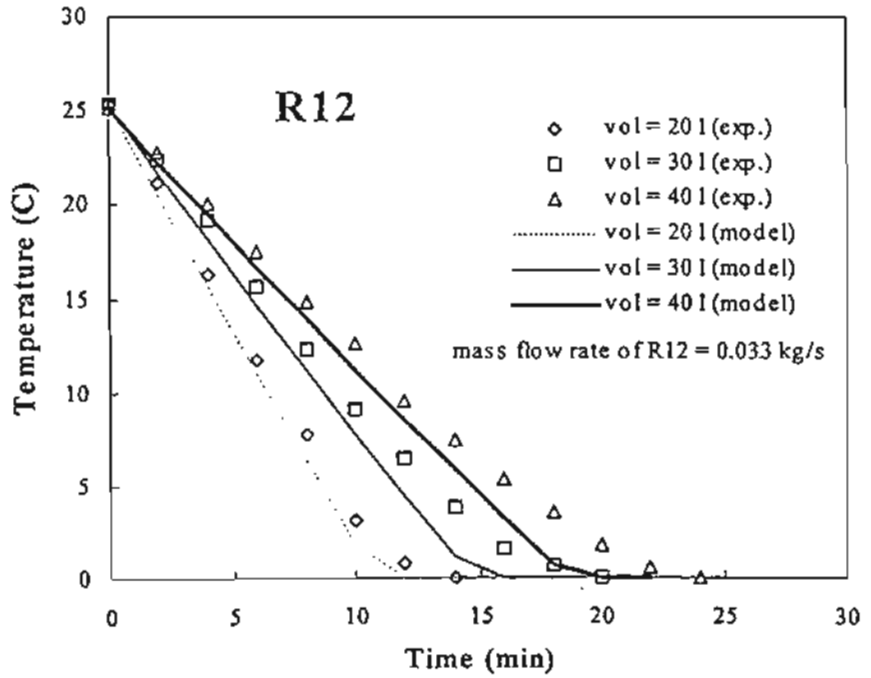

Figure 4 Comparison of water temperatures in the storage tank between the experiment with the lump model at various amounts of water; mass flowrate of refrigerant = 0.033 kg/s.

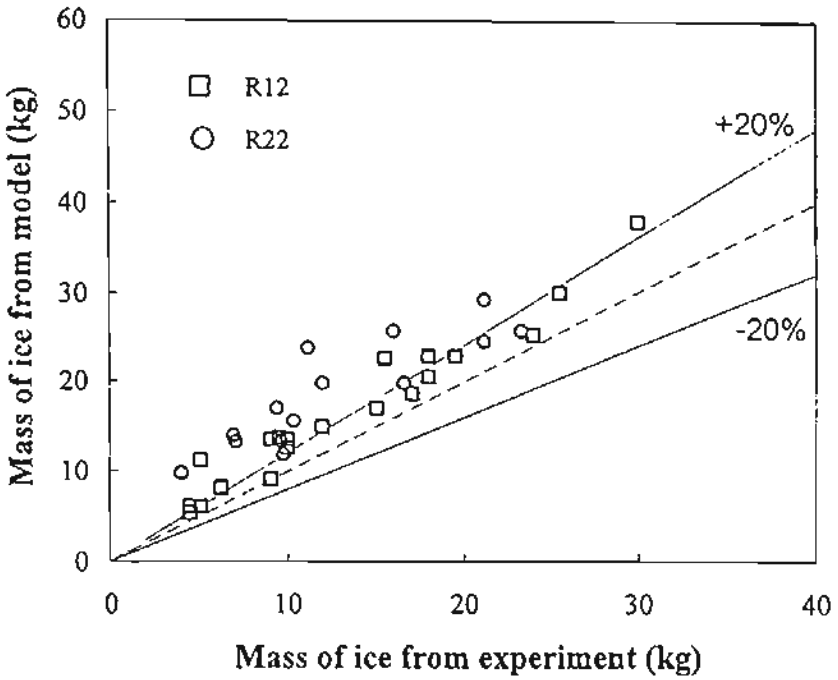

Figure 5 Comparison of amount of ice in the storage tank from the experiment with the model.

Figure 6 shows the volumetric heat transfer coefficient (U_v) of the heat exchange in the storage tank which can be calculated from

$$U_v = \frac{\dot{m}_r (h_{ro} - h_{ri})}{V(T_w - T_{ri})}, \qquad [6]$$

where V is the volume of water in a storage tank.

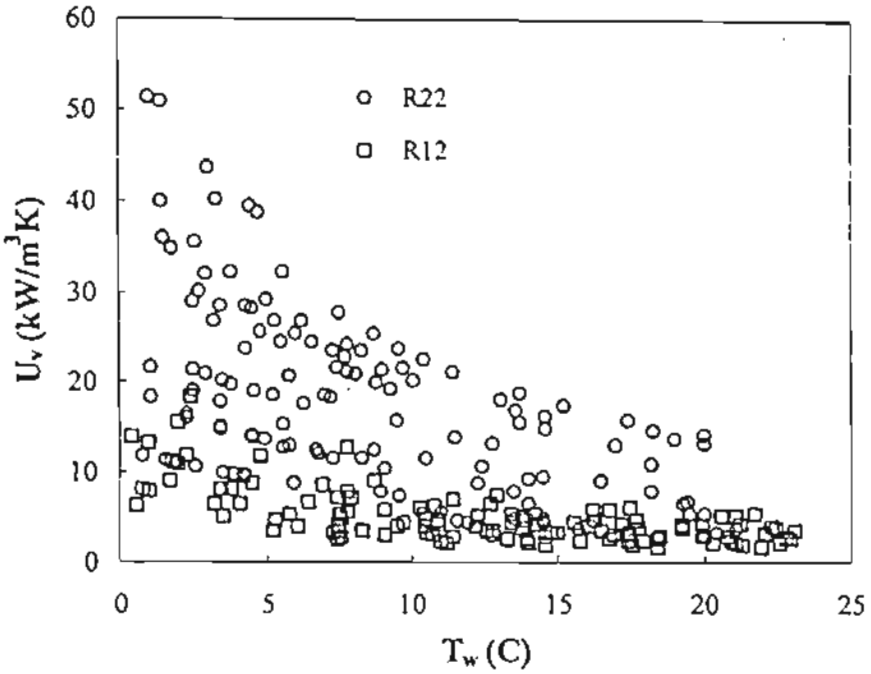

Figure 6 Volumetric heat transfer coefficient of the direct contact evaporator at various conditions.

From Figure 6 it is found that the volumetric heat transfer coefficient increases when the temperature of water decreases. As the temperature of water nearly freezing point, the volumetric heat transfer coefficient increases drastically. It is found that the range of the volumetric heat transfer coefficient is around 2-16 kW/m^3 in case of R12 and around 2-52 kW/m^3 in case of R22. These values are low compared to the results of Blair et al. [3] (122 kW/m^{3}K; R113-water), Sideman and Gat [4] (180 kW/m^{3}K; pentane-water) and slightly high compared to that of Goodwin et al. [5] (3-8 kW/m^{3}K; pentane-water). The differences possibly arise from many reasons. Firstly is the method of testing, Blaire et al.[3], Sideman and Gat [4] and Goodwin et al. [5], inject the refigerant into the continuous flow of water (Figure 7) while the present experiment uses the stagnant water (no flow). In the previous studies, the water temperature is

nearly constant while the water temperature in our experiment continually decreases. Moreover, in the previous works, there are no data on the temperature difference of the dispersed and continuous phases. From Equation 6, if this temperature difference is smaller, higher volumetric heat transfer coefficient is obtained.

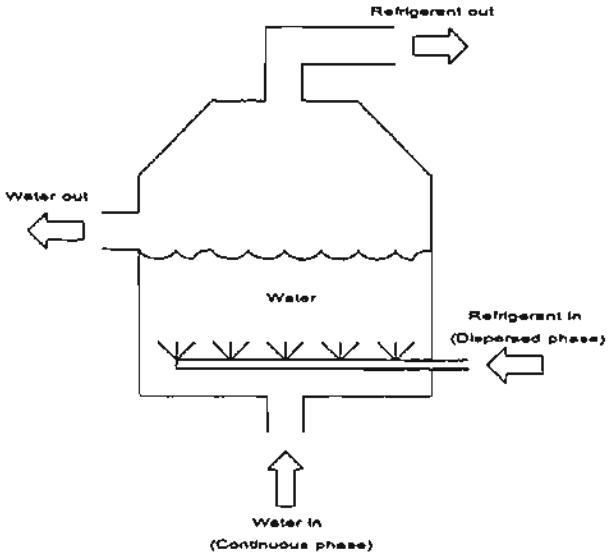

Figure 7 The direct contact heat exchange technique with dispersed and continuous phase.

The second reason is the effect of the size of the storage tank. Table 2 shows the comparison of the testing conditions from our study with the other researchers. The storage tank diameters (or the tank capacities) of Blair et al. [3] and Sideman and Gat [4] are smaller compared to the present study and that of Goodwin et al. [5]. From Equation 6, the value of water in a storage tank plays an important role to the volumetric heat transfer coefficient. Lower amount of water in the tank will get higher volumetric heat transfer coefficient. This is the reason why the volumetric heat transfer coefficient of our study and Goodwin et al. [5] are lower than those of Blair et al. [3] and Sideman and Gat [4].

Table 2 Comparison of working conditions of direct contact heat transfer systems.

	Present study	Sideman and Gat	Blair et al.	Goodwin et al.
U_v (kW/m^{3}K)	2-16, 2-52	180	122	3-8
Dispersed phase	R12, R22	pentane	R113	pentane
Mass flow rate of dispersed phase (kg/s)	0.02-0.08	0.022	0.023	1.90
Mass flow rate of continuous phase (kg/min)	-	0.042	0.101	17.1
Diameter of storage tank (m)	0.30	0.07	0.095	0.61

Heat Transfer Correlation of the Direct Contact Evaporator

The parameters affecting the heat transfer of the direct contact evaporator could be grouped into the dimensionless parameters which could be listed in terms of Stanton number, Stephan number and Prandtl number, where

$$St = \frac{U_v V}{(\dot{m} Cp)_r}, \qquad [7]$$

$$Ste = \frac{Cp_w (T_w - T_n)}{\lambda_w}, \qquad [8]$$

$$Pr = \left(\frac{Cp\mu}{k}\right)_r. \qquad [9]$$

St is Stanton number, *Ste* is Stephan number and *Pr* is Prandtl number. The dimensionless group could be expressed as

$$St = f\left(Ste\ Pr^{0.25}\left(\frac{p}{Pa}\right)^{-1}\right). \qquad [10]$$

Note that P/Pa is the pressure ratio of the pressure in the storage tank and that of the surrounding ambient.

Figure 8 shows the relation of the dimensionless parameters when using R12 and R22. St increases when $StePr^{0.25}(P/Pa)^{-1}$ is decreased. Lower Ste means the temperature difference (T_w-T_{ri}) is reduced which results in higher values of U_v and St. The values of U_v and St are very high when the water temperature is close to the freezing point. Lower the value of P results in lower the refrigerant temperature then there is a bigger difference between the water and the refrigerant temperatures thus higher heat transfer is obtained.

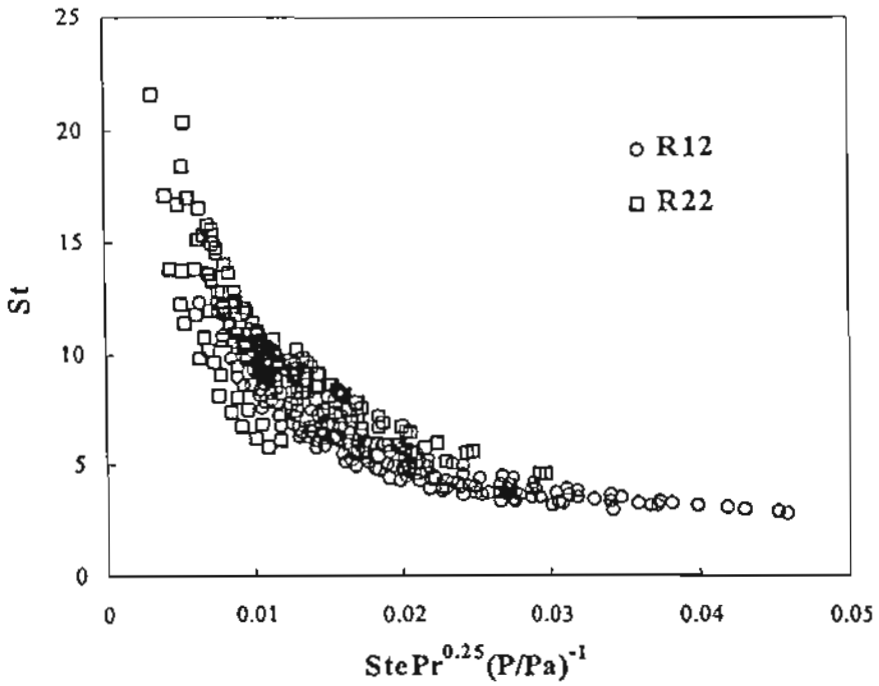

Figure 8 The relation of the dimensionless parameters.

By fitting all the experimental data the dimensionless group could be expressed as

$$St = 0.1967\left(Ste\ Pr^{0.25}\left(\frac{P}{Pa}\right)^{-1}\right)^{-0.8445} \quad . \qquad [11]$$

Figure 9 also shows the comparison of the Stanton number calculated from Equation (11) and the experimental data. It is found that the model can predict the experimental data within ± 30% error.

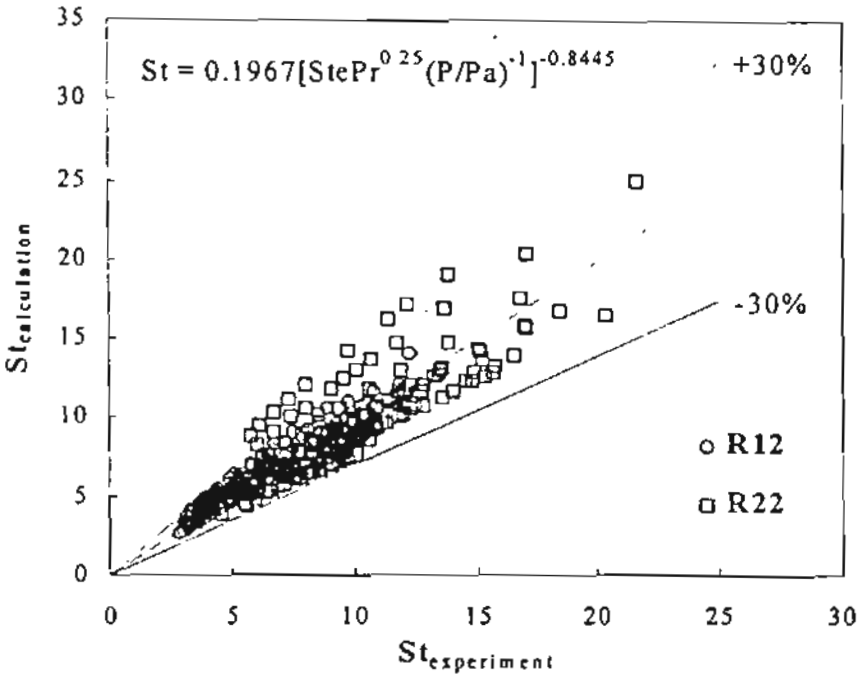

Figure 9 Comparison of *St* calculated from Equation 11 with the experimental data.

CONCLUSION

The direct contact heat transfer technique with injection of refrigerant gives high heat transfer rate. The lump model can be modified to predict the temperature of the water during the sensible heat period and the amount of ice during latent heat period. The relation of the dimensionless parameters is expressed and it can be used to predict the experimental value quite well.

Acknowledgement

The authors gratefully acknowledge the financial support provided by Thailand Research Fund (TRF) for carrying out this study. Sincere thank is also extended to Mr. Tanai Chatakanonda and Mr. Piya Na Bangchang for their valuable data.

REFERENCES

1. Electricity Generating Authority of Thailand (EGAT), Thailand power development plan PDP 1997-01, System Planing Department, Bangkok, Thailand, 1997 (in Thai).
2. Vorayos N., Development of a prototype of an ice thermal energy storage with direct contact evaporator, M.Phil. Thesis, The Joint Graduate School of Energy and Environment, King Mongkut's University of Technology Thonburi, Bangkok, Thailand, 2001.
3. Blair C.K., Boehm R. and Jacobs H., Heat transfer characteristics of a direct contact volume type boiler, ASME, 1976; 76-HT-26.
4. Sideman S. and Gat Y., Direct-contact heat transfer with change of phase: Spray column studies of a three phase heat exchanger, AIChE Journal, 1966;12(3):296-303.
5. Goodwin P., Cobin M. and Boehm R., Evaluation of the flooding limits and column, ASME National Heat Transfer Conference, Denver, 1985; 85-HT-49.
6. Subbaiyer S., Andhole T.M. and Helmer W.A., Computer simulation of a vapor-compression ice generator with direct contact evaporator, ASHRAE Transactions, 1991; Part 1(3448): 118-126.
7. Kiatsiriroat T., Na Thalang K. and Dabbhasuta S., Ice formation around a jet stream of refrigerant, Energy Conversion & Management, 2000; 41: 213-221.

8. Nuntaphan A., Performance analysis of a refrigeration cycle using a direct contact evaporator, M.Eng. Thesis, Department of Mechanical Engineering, Chiang Mai University, Chiang Mai, Thailand, 1998.

9. Chatakanonda T. and Na Bangchang P., A R22 refrigeration unit with direct contact evaporator, Senior Project, Department of Mechanical Engineering, Chiang Mai University, Chiang Mai, Thailand, 1999.

Nomenclature

A	area (m^2)
Cp	specific heat (kJ/kgK)
h	enthalpy (kJ/kg)
k	thermal conductivity (kW/mK)
m	mass (kg)
$\dot{m}$	mass flowrate (kg/s)
P	pressure (Pa)
Pa	ambient pressure (Pa)
Pr	Prandtl number
T	temperature (°C)
t	time (s)
U_v	volumetric heat transfer coefficient (kW/m^3K)
St	Stanton number
Ste	Stephan number
V	volume (m^3)

Greek symbols

λ latent heat of formation (kJ/kg)

μ dynamic viscosity (Pa.s)

Subscripts

i inlet

l liquid

o exit

r refrigerant

t storage tank

w water

Feasibility of Using Ice Thermal Energy Storage with Direct Contact Evaporator in an Office Building

T. Kiatsiriroat
Department of Mechanical Engineering
Chiang Mai University, Chiang Mai 50200, Thailand
N. Vorayos
Joint Graduate School of Energy and Environment
King Mongkut's University of Technology Thonburi
Bangkok 10140, Thailand
A. Nuntaphan
South East Asia Center for Training in Energy for Development
Electricity Generating Authority of Thailand
Mae Moh, Lampang 52220, Thailand

Abstract - In this research, an ice thermal energy storage with direct contact evaporator has been studied by applying to an office located in Chiang Mai University, Chiang Mai, Thailand. The system consists of two cycles, basic chilled water and ice storage. The mathematical models for main components composing of compressor, condenser, expansion valve, water chiller and direct contact evaporator are developed and the system simulation is created. Evidently from the results, the simulation agrees well with the experiments with 5% error. Different options of the energy storage types, full storage, partial storage and demand-limited storage, have been considered. The simulation also indicates that the demand-limited storage design system is the most appropriate storage option for the selected office. Under this operating condition, the system can shift 39.3% of peak electricity demand from on-peak period to off-peak period. Therefore, 33.8% of electricity charge is saved comparing to those of the conventional system.

Keywords: Ice thermal energy storage, direct contact heat transfer technique, system simulation, economic feasibility

Submitted to **Energy Research – The International Journal**

Address of Correspondence and Proof:
Prof. Dr. Tanongkiat Kiatsiriroat
Department of Mechanical Engineering, Faculty of Engineering,
Chiang Mai University, Chiang Mai 50200, Thailand.
Tel: 6653-944144 Fax: 6653-944145 E-mail: *tanong@dome.eng.cmu.ac.th*

1. INTRODUCTION

In tropical countries, electricity requirement is mainly caused by air conditioning system due to high ambient temperature. In Thailand, the peak electricity demand increases 12% annually and occurs during the day and in the evening [1]. Instead of constructing new power plants to meet the increment, the Electricity Generating Authority of Thailand introduces electricity tariff which charges the consumers with high premium rate for the energy consumed during the on-peak period and low rate during the off-peak period to achieve uniform load factor. Ice thermal energy storage (ITES) is an energy management technique that is becoming an attractive alternative for buildings to avoid the high electricity demand charge for space cooling. The principle of this technique is that the coolness is produced at night in form of ice stored in a well-insulated storage. The coolness could be used to supply the cooling requirement during the daytime. At present, the most common ITES systems used is the ice-on-coil storage system of which ice is formed on the surface of the cooling coil submerged in the water. There are two main problems, big space for handling the evaporator coil is needed and high thermal resistance is obtained due to the low thermal conductivity of the ice forming on the coil [2,3]. To overcome these problems, the application of direct contact heat transfer technique has been interested [4-6]. In this paper, the mathematical models of the main components and the system simulation of the ITES unit with direct contact evaporator using R12 as working fluid have been developed. The paper also investigates in the application of the system for an office in Chiang Mai, Thailand. The concentrated storage options are full storage, partial storage and demand-limited storage.

2. COOLING LOAD AND ITES CATEGORIES

The ITES system with direct contact evaporator considered in this research work is operated to support the cooling requirement of the selected office in Chiang Mai University. The cooling area of the office is 178.75 m^2 of which the cooling load profile based on the data in year1998 is shown in Fig. 1.

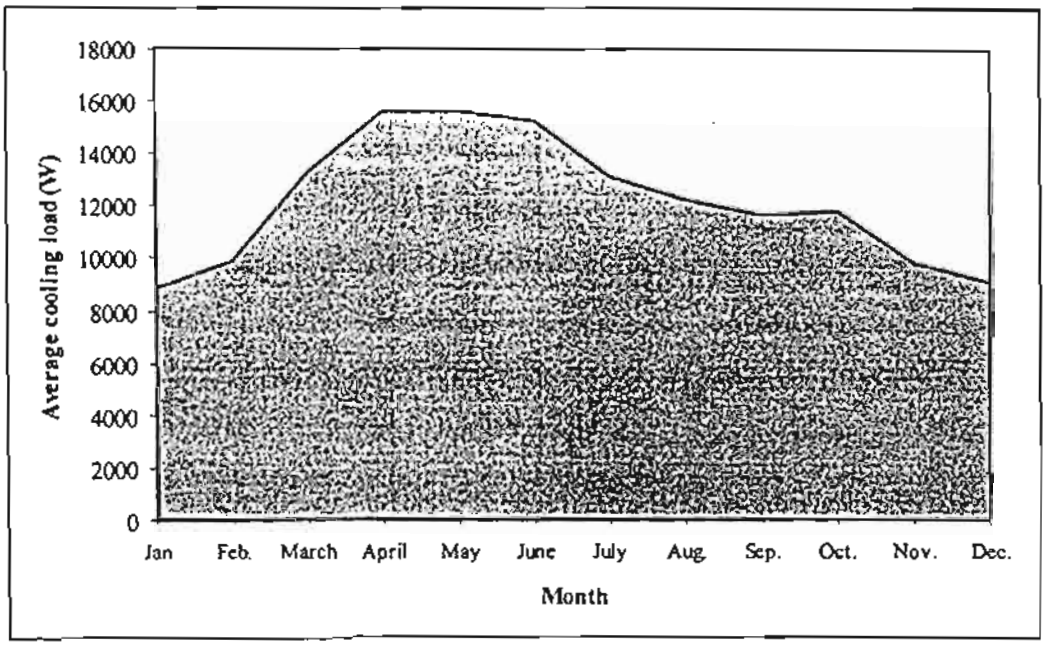

Fig. 1. The cooling load profile of the selected office during the year 1998.

The electricity consumption of the office during the year is 27163 kW-hr/year. In this case, the air conditioning system consumes 45% of total energy. Due to the load profile shown in Fig. 2, the maximum energy demand is 24.7 kW. It includes 9.7 kW of the electricity demand for cooling system and 15 kW for other purposes. The electricity tariff used to calculate the electricity charge of the office or TOU rate is given in Table 1[1].

Table 1. Electricity cost (TOU Rate)

Demand Charge (Baht/kW)	Energy Charge (Baht/kW-hr)			Service Charge (Baht/month)
1*	1*	2*	3*	
102.80	1.5349	0.6671	0.6062	400

1*	Monday – Saturday	09.00 – 22.00 (On-peak)
2*	Monday – Saturday	22.00 – 09.00 (Off-peak)
3*	Sunday	00.00 – 24.00 (Off-peak)

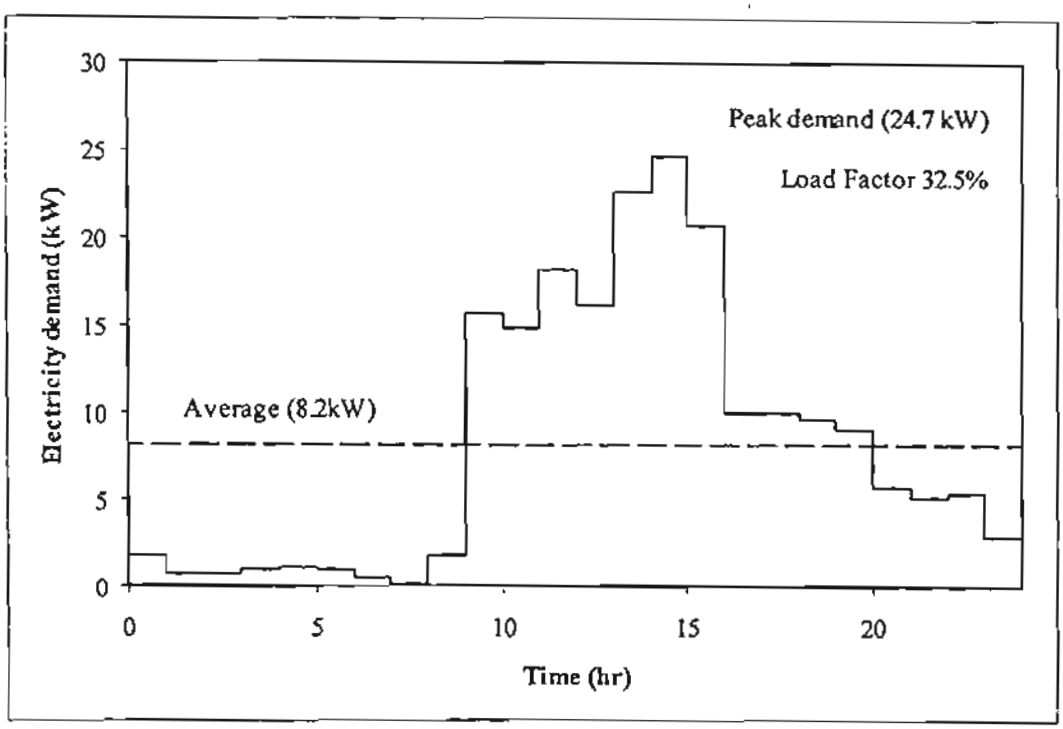

Fig. 2. The profile of electricity demand of the office during the design day.

To find out the appropriate storage option, different ITES designs have been investigated which are as follows:

Category 1. Conventional design (no ice storage). The entire cooling load requirement of the office is supported by a chilled water system operating during the occupancy period.

Categories 2-5. Partial storage design. The cooling load is divided into two parts. The first part called the base load which is supported by the chiller unit during the occupancy time and the excess is supported by the ice in storage tank produced by an ITES system operating during the nighttime. The portion of the base load for the categories 2-5 are 75%, 60%, 40% and 20%, respectively.

Categories 6. Demand-limited storage design. The peak electricity demand of the office is limited at 15 kW. In this category, the chilled water system runs during the occupancy period except the hours that the total electricity demand of the office reaches the limited value.

Category 7. Full storage design. The entire cooling load requirement is supported by the ice storage system. The chiller unit is not provided in this case.

3. THE ICE THERMAL ENERGY STORAGE CYCLES

The space cooling of the office is normally supported by a conventional chiller unit of about 5 TR (18 kW). To modify the unit with the ITES system, another 2 TR (7 kW) refrigeration unit is used for the ice storage unit. The schematic diagram of the air conditioning system with the ITES unit is shown in Fig. 3.

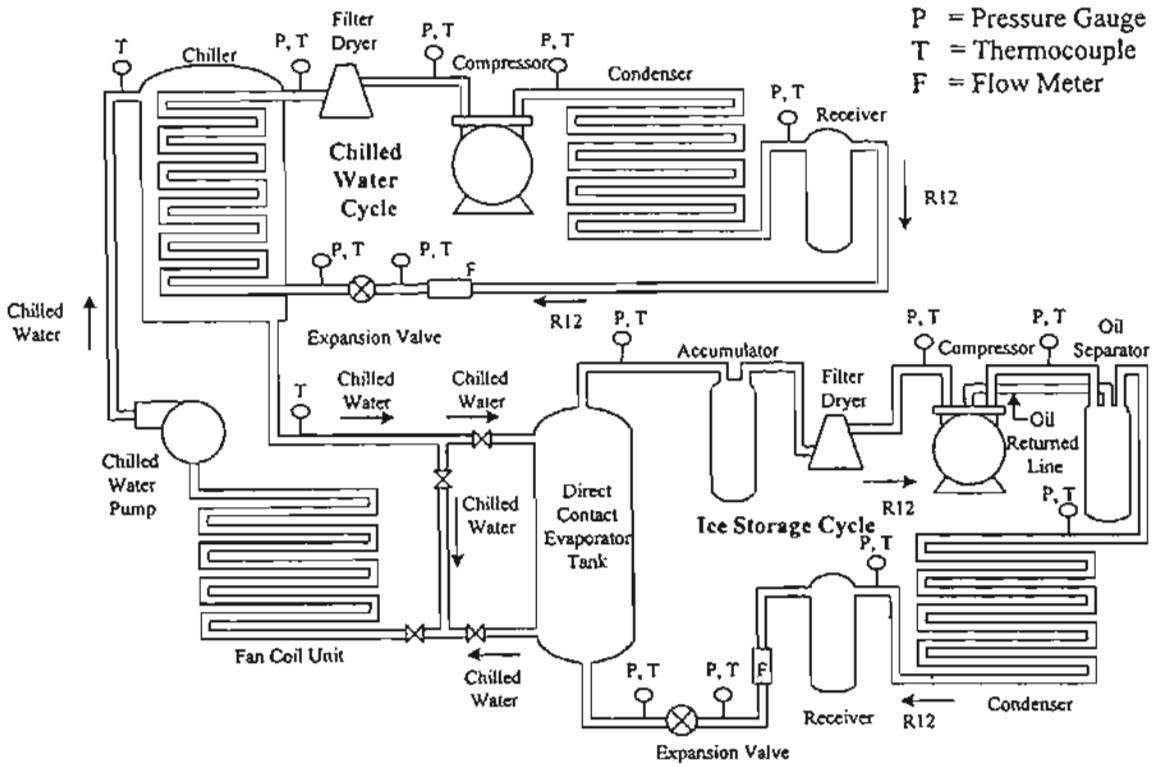

Fig. 3. Schematic diagram of the ice thermal energy storage.

The system consists of two main cycles, the ITES cycle and the chilled water cycle. During the ice formation process, the ITES cycle normally runs during the off-peak period. R12 refrigerant is injected through the expansion valve then the pressure and the temperature of R12 decrease. The low temperature R12 exchanges heat with water in the storage tank directly and it leaves the tank as vapor and turns back to the condensing unit. During the on-peak period, for partial and demand-limited storages, the base-cooling load is supported by the chilled water cycle and the excess is supported by the coolness stored in the storage tank. In case of full storage, all cooling load requirement is supported by the stored coolness.

The mathematical model of each system is separately investigated as follows:

3.1 Ice Thermal Energy Storage (ITES) System

A standard 2 TR (7 kW) open-type reciprocating compressor is used in the ice storage cycle with a direct contact evaporator. To formulate the mathematical models of the system, the refrigerant (R12) mass flow rate is varied from 0.02 – 0.09 kg/s and the compressor speed is controlled at 7.1, 9.5 and 11.8 rps. The characteristic models of main components in the system are created from the experimental data as followings:

Compressor Model

Kiatsiriroat et al. [7] generates a mathematical model of a reciprocating compressor, which is modified from Stoecker [8] as

$$\frac{P_{cp,i}}{P_{cp,o}} = f\left[\frac{m_r T_{cp,o}^{0.5}}{P_{cp,o}}, N\right], \tag{1}$$

where N is the compressor speed in rps, m_r is the refrigerant mass flow rate in kg/s, $T_{cp,o}$, $P_{cp,i}$ and $P_{cp,o}$ are outlet temperature and pressures at the inlet and outlet of the compressor in K and MPa, repectively.

The correlation can be deduced from the experimental results as

$$\frac{P_{cp,i}}{P_{cp,o}} = \left[\begin{array}{l}\left(-0.0015N^2 - 0.0087N + 0.3003\right)\left[\dfrac{m_r T_{cp,o}^{0.5}}{P_{cp,o}}\right] \\ +\left(0.0022N^2 - 0.0581N + 0.5824\right)\end{array}\right] \tag{2}$$

The pressure ratio of the compressor can be additionally calculated from

$$\frac{P_{cp,i}}{P_{cp,o}} = \left(\frac{T_{cp,i}}{T_{cp,o}}\right)^{k/(k-1)} \tag{3}$$

where k is the polytropic index depending on the refrigerant mass flow rate. The relation between the flow rate and the index can be expressed as

$$k = 1.9584\, m_r + 1.1503\,. \tag{4}$$

Condenser Model

The mathematical modeling of air-cool condenser could be modified from

$$\frac{(T_{a,o} - T_a)}{(T_{cd,i} - T_a)} = f\left[\frac{(UA)_{cd}}{m_a C_{pa}}\right] \tag{5}$$

where T_a is ambient temperature in °C, $T_{a,o}$ is the outlet air temperature in °C, $T_{cd,i}$ is inlet refrigerant temperature in °C, $(UA)_{cd}$ is overall heat transfer coefficient of condenser in kW/K, m_a is air mass flow rate in kg/s and C_{pa} is specific heat of air in kJ/kg.K.

Deduced from the experiment, the characteristic equation of the condenser can be expressed as

$$\frac{T_{a,o} - T_a}{T_{cd,i} - T_a} = \frac{0.2723(UA)_{cd}}{m_a C_{pa}} + 0.0107\,. \tag{6}$$

Expansion Valve Model

The expansion valve is operated manually to control the refrigerant mass flow rate and the pressure of the system. The relation between the pressure ratio at the valve and the refrigerant mass flow rate can be modified from

$$\frac{P_{exo}}{P_{exi}} = f(m_r, N). \tag{7}$$

where the characteristic equation can be experimentally expressed as

$$\frac{P_{ex,o}}{P_{ex,i}} = \begin{bmatrix} (1.5134N^2 - 32.0125N + 148.8285)m_r^2 \\ +(-0.1020N^2 + 2.0160N - 5.8329)m_r \\ +(0.0032N^2 - 0.0824N + 0.7113) \end{bmatrix}. \tag{8}$$

Direct Contact Evaporator Model

The mathematical model for the direct contact evaporator is formulated by a lump model [6]. Using the energy balance, the thermal characteristics of the water in the tank can be expressed as

$$\frac{d}{dt}(M_w h_w) + M_t C_t \frac{dT}{dt} = m_r(h_{ev,i} - h_{ev,o}) + (UA)(T_a - T_w). \tag{9}$$

As shown in the equation, the first three terms relate to the enthalpy change rates of the water, the container and the refrigerant, respectively. The last term relates to the external heat gain from the surrounding ambient. In this study, the direct contact evaporator is well insulated, the external heat gain then can be neglected. The water temperature of the water inside the tank changes in two steps according to two related processes, which are sensible heat process and ice formation process. The characteristic equations of the direct contact evaporator during the sensible heat process and the ice formation process can be expressed in the following equations, respectively as

$$T_w^{t+\Delta t} = T_w^t + \frac{m_r(h_{ev,i} - h_{ev,o})\Delta t}{M_t C_{pt} + M_w C_{pw}}, \tag{10}$$

and

$$M_{ice} = \frac{m_r(h_{ev,o} - h_{ev,i})\Delta t}{L}. \tag{11}$$

Due to the long length of the pipes between the evaporator unit, the compressor and the condenser, the heat gain and loss can not be ruled out. From the preliminary study, the heat gain

between the low temperature refrigerant flowing inside the pipes from the evaporator to the compressor and the surrounding ambient can be characterized as

$$m_r C_{pr}\left(T_{cp,i} - T_{ev,o}\right) = f\left(T_a - \left(\frac{T_{ev,o} + T_{cp,i}}{2}\right), m_r\right) \tag{12}$$

The equation can be expressed from the experimental results as

$$m_r C_{pr}\left(T_{cp,i} - T_{ev,o}\right) = \begin{bmatrix} \left(-0.4132m_r^2 + 0.0409m_r - 0.0012\right)\left(T_a - \left(\frac{T_{ev,o} + T_{cp,i}}{2}\right)\right)^2 \\ + \left(6.0055m_r^2 - 0.3648m_r + 0.0448\right)\left(T_a - \left(\frac{T_{ev,o} + T_{cp,i}}{2}\right)\right) \\ + \left((-38.4022)m_r^2 + 6.243m_r - 0.2699\right) \end{bmatrix}. \tag{13}$$

As the high temperature refrigerant flows through the pipe between the compressor and condenser, the heat loss occurs and can be characterized as

$$m_r C_{pr}\left(T_{cp,o} - T_{cd,i}\right) = f\left(\left(\frac{T_{cp,o} + T_{cd,i}}{2}\right) - T_a, m_r\right). \tag{14}$$

The heat loss characteristic is experimentally observed. The empirical relation between this loss and aforementioned relevant parameters is deduced as

$$m_r C_{pr}\left(T_{cp,o} - T_{cd,i}\right) = \begin{bmatrix} \left(-0.0001\right)\left(\left(\frac{T_{cp,o} + T_{cd,i}}{2}\right) - T_a\right)^2 \\ \left(1.607m_r^2 - 0.0298m_r - 0.0146\right)\left(\left(\frac{T_{cp,o} + T_{cd,i}}{2}\right) - T_a\right) \\ + \left(-20.432m_r^2 + 1.9399m_r - 0.293\right) \end{bmatrix}. \tag{15}$$

Observed from the results, there is a pressure drop across the condenser which can be expressed as

$$P_{cd,o} = P_{cd,i} - 0.034 \tag{16}$$

where $P_{cd,i}$ and $P_{cd,o}$ are the pressure at the inlet and outlet of condenser in MPa.

3.2 Chilled Water System.

A standard 5 TR (18 kW) vapor-compressor refrigeration system is simulated under steady-state conditions to produce the chilled water to support the cooling load requirement. The compressor is usually worked at constant full speed. The modeling of each main component is developed as the followings:

Compressor Model

The mathematical model of the compressor can be generated [7] as

$$\frac{P_{cp,i}}{P_{cp,o}} = f\left[\frac{m_r T_{cp,o}^{0.5}}{P_{cp,o}}, N\right], \tag{1}$$

and

$$\frac{P_{cp,i}}{P_{cp,o}} = f\left[\frac{m_r T_{cp,i}^{0.5}}{P_{cp,i}}, N\right]. \tag{17}$$

From eqs. 1 and 17, the characteristic equations of the compressor in the chilled water system can be experimentally deduced as

$$\frac{P_{cp,i}}{P_{cp,o}} = 0.0973\left(\frac{m_r T_{cp,i}^{0.5}}{P_{cp,i}}\right) + 0.0663, \tag{18}$$

and

$$\frac{P_{cp,i}}{P_{cp,o}} = 0.0873\left(\frac{m_r T_{cp,o}^{0.5}}{P_{cp,o}}\right) + 0.1088. \tag{19}$$

The relation between the refrigerant mass flow rate and the polytropic index of the compressor can be expressed as

$$k = -2.1397 m_r^2 + 0.4896 m_r + 1.1867. \tag{20}$$

Condenser Model

A shell and tube heat exchanger having circulating water as a coolant is used as a condenser to extract heat from the refrigeration system. The extracted heat is calculated from

$$Q_{cd} = m_r\left(h_{cd,i} - h_{cd,o}\right). \tag{21}$$

Q_{cd} is the rate of heat extraction in kW, m_r is refrigerant mass flow rate in kg/s and $h_{cd,i}$ and $h_{cd,o}$ are the enthalpies at the inlet and the outlet of the condenser (kJ/kg).

Expansion Valve Model

The mathematical modeling of the manual-controlled expansion valve can be modified from eq. 7 and expressed as

$$\frac{P_{ex,o}}{P_{ex,i}} = -20.114m_r^2 + 3.5432m_r + 0.1291. \tag{22}$$

Chiller Model

The water chiller used in this case is a shell-and-tube flow type of which the relevant heat transfer rate is calculated from

$$Q_{ch} = m_r\left(h_{ch,o} - h_{ch,i}\right), \tag{23}$$

or

$$Q_{ch} = m_w C_{cpw}\left(T_{w,i} - T_{w,o}\right), \tag{24}$$

and

$$Q_{ch} = (UA)_{ch}\left[\frac{\left(T_{w,i} - T_{ch,o}\right) - \left(T_{w,o} - T_{ch,i}\right)}{\ln\left[\frac{T_{w,i} - T_{ch,o}}{T_{w,o} - T_{ch,i}}\right]}\right], \tag{25}$$

where $(UA)_{ch}$ is overall heat transfer coefficient of chiller in kW/K.

It is observed that there is a pressure drop across the condenser and the chiller which can be expressed in terms of the pressure ratio as

$$\frac{P_{cp,i}}{P_{cp,o}} = 0.7733\left[\frac{P_{ex,o}}{P_{ex,i}}\right] - 0.0194. \quad (26)$$

3.3 System Simulation

With the mathematical modeling of each component in the system, the simulation is created to determine the energy consumption of the system at various possible combinations of the conventional chilled water system and the ice thermal energy storage (ITES) system. The computational steps are shown in Fig.4.

As shown in Fig.4, the simulation consists of two parts, chilled water system and ITES system. The input parameters of the simulation are the total cooling load, Q_{load}; the compressor speed of the ice storage system, N_{dc}; the mass flow rate of the refrigerant for the ice storage system, $m_{r,dc}$; the initial temperature of water in the storage tank, T_{wi}; the ambient temperature, T_{amb} and the properties of the working fluid.

The cooling load is divided to be $Q_{load,ac}$ for the chilled water system and $Q_{load,dc}$ for the ice storage system. For the chilled water system, the trial and error technique has been carried out to find the suitable mass flow rate of the refrigerant at a given cooling load and the power input of the compressor is also the output result. The equations used to calculate the properties of R12 refrigerant are [9]:

For the saturated conditions,

$$\ln(P_{sat} \times 10) = -15.6 + 8.96\left(\frac{T_{sat} + 273.15}{100}\right) - 1.038\left(\frac{T_{sat} + 273.15}{100}\right)^2 \quad (27)$$

$$h_f = -239.8 + 100.6\left(\frac{T_{sat} + 273.15}{100}\right) \quad (28)$$

$$h_g = 187.28 + 0.4722(T_{sat}) \quad (29)$$

The suffixes "*f*" and "g" refer to saturated liquid and saturated gas conditions, respectively and the suffix "*sat*" refers to saturated condition.

For superheat conditions,

$$h = 173.52 + 13.01(\ln(P \times 10)) + (0.57 + 0.0826 \ln(P \times 10))(T - T_{sat}) \qquad (30)$$

P and T are pressure and temperature in MPa and K, respectively and h is the specific enthalpy in kJ/kg.

For the ice storage part, the calculation method of each component is similar to that of the chilled water system. Note that, the refrigerant temperature leaving the ice storage tank is close to the water temperature in the tank because of high turbulence due to the refrigerant injection. When the temperature of water is higher than the freezing point, the calculation is in sensible heat mode. As the water temperature is the same as the freezing point, the latent heat mode is applied. The outputs of this part are the power consumption at the compressor, the heat transfer rate of the direct contact evaporator and the time consumed for producing ice.

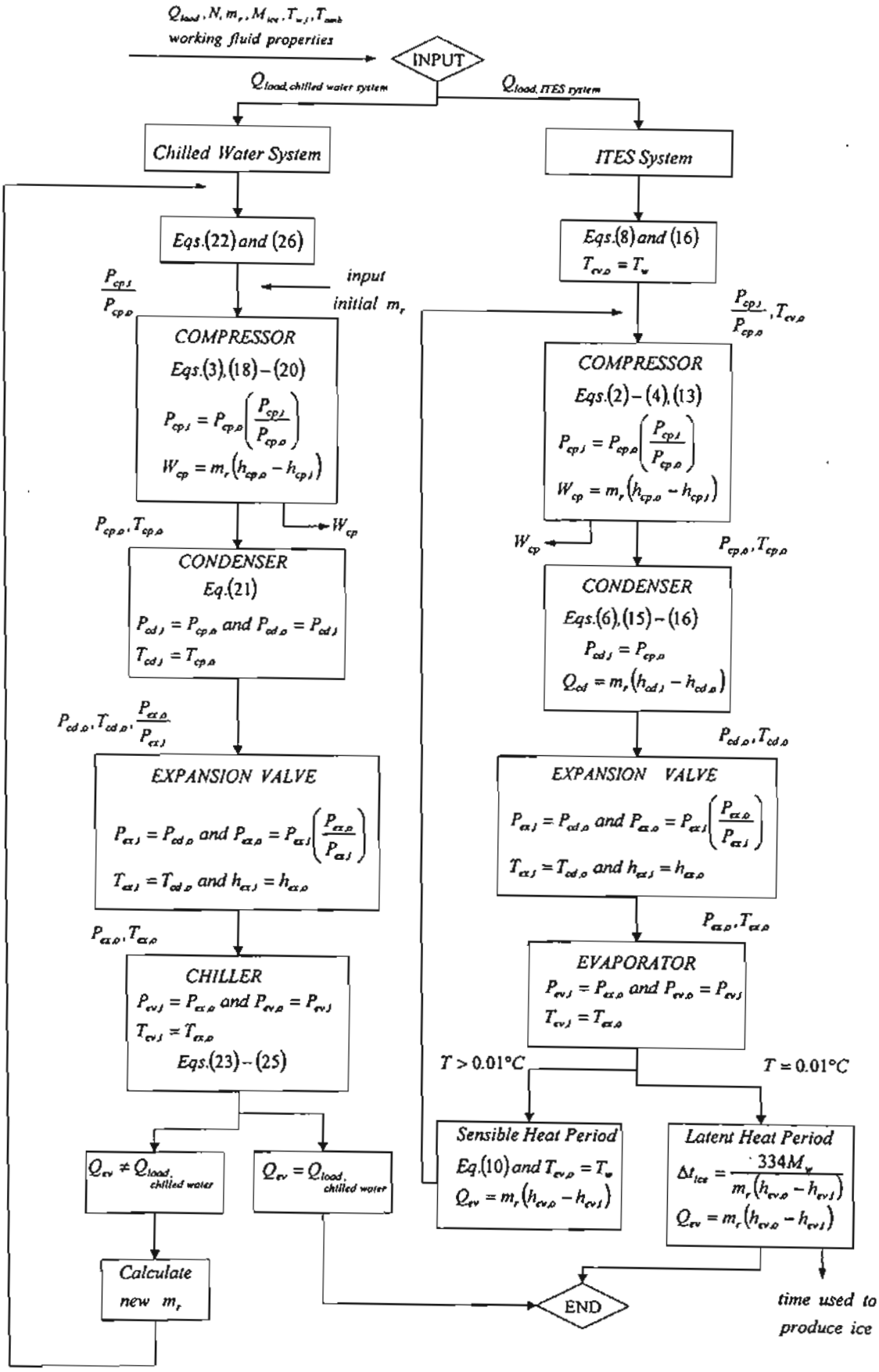

Fig. 4. Information flow diagram of the system simulation.

3.4 Simulation Results

Chilled Water System

With a given cooling load, and ambient temperature, the compressor work of the chilled-water system could be evaluated. The results from the simulation are compared to those of the experiments as illustrated in Fig. 5.

It is noted that the values from the simulation program are close to the experimental results within 5% error.

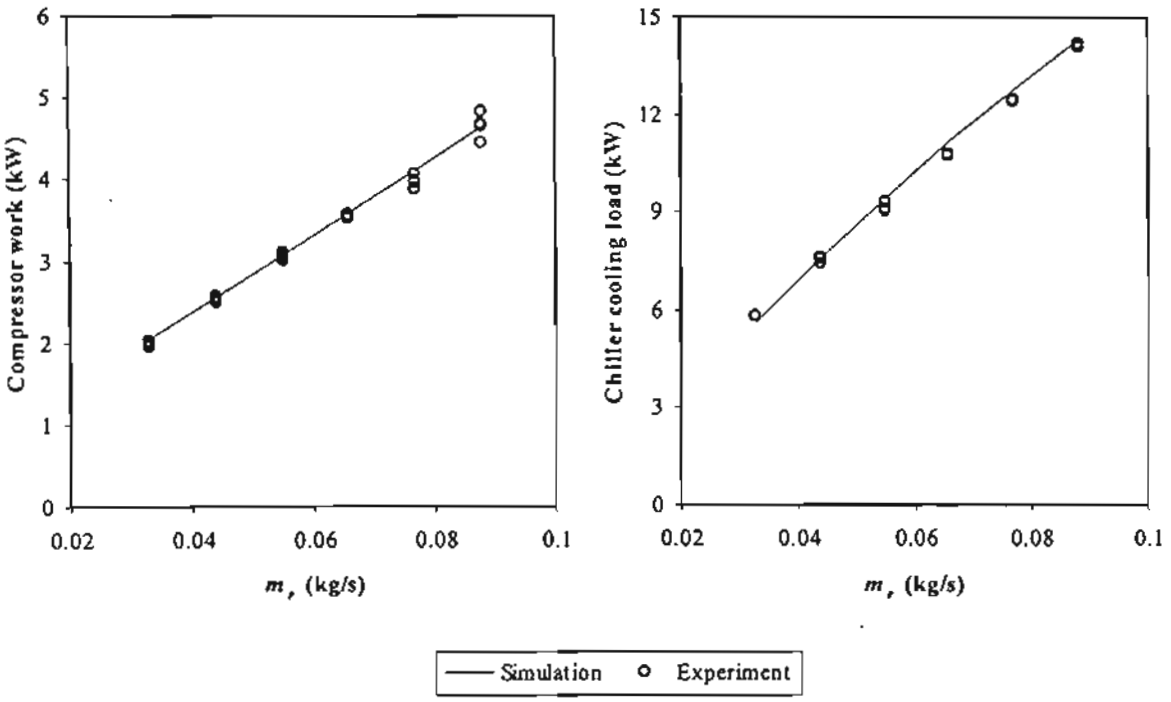

Fig. 5. Compression work and cooling load of the chilled-water system.

ITES System

(a) Ice formation process

For the ice storage simulation, the compressor work, the heat transfer rate at the direct contact evaporator the time used to produce ice and the amount of ice are evaluated. Fig. 6 shows the results of the compression work and the cooling capacity in the direct contact evaporator. The simulated results are in good agreement with those of the experiments within 5 % error.

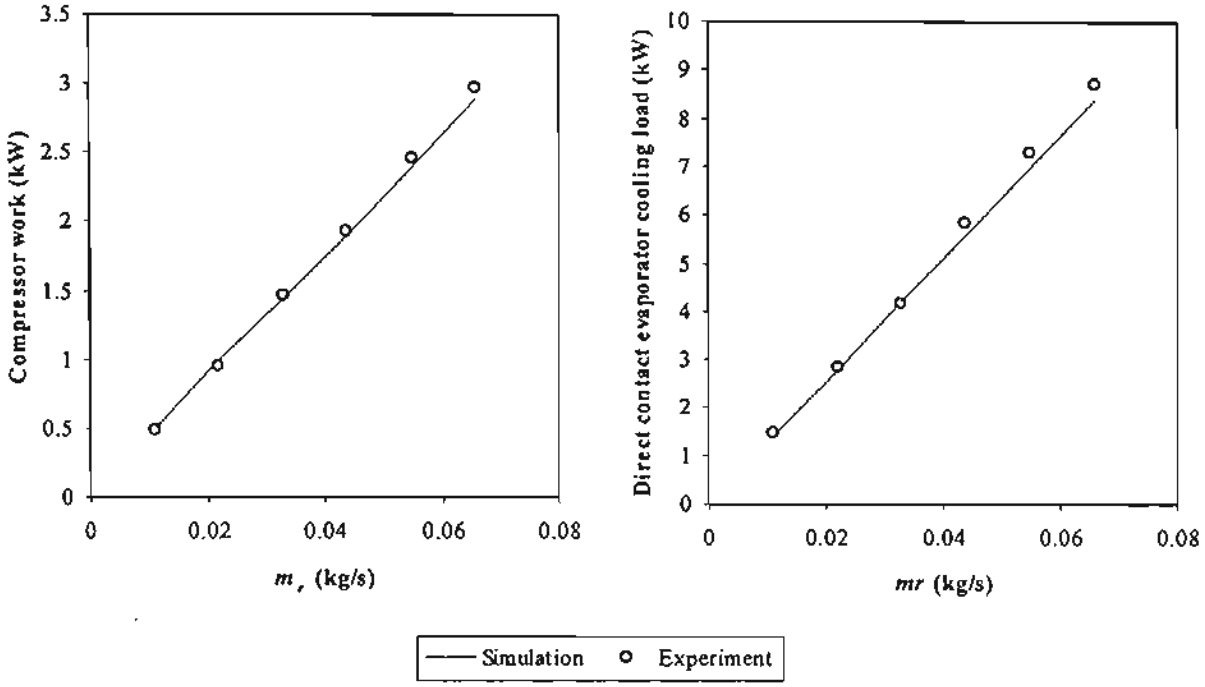

Fig. 6. Compression work and evaporator cooling load of the ITES system.

Table 2 shows the time used to generate ice and the amount of ice formed in the evaporator-storage tank. The results agree quite well with those of the experiments.

Table 2.The amount of ice formed and time used.

Mass of water in storage tank (kg)	m_r (kg/s)	N (rps)	Initial water temp. (°C)	T_{amb} (°C)	Produced ice (kg) (sim.)	Time (hr) (sim.)	Produced ice (kg) (exp.)	Time (hr) (exp.)
250	0.077	11.8	18.0	29.2	250	3.66	212	3.59
250	0.100	11.8	16.5	30.2	250	3.11	209	3.23
300	0.066	11.8	15.0	28.5	300	5.01	272	4.98
300	0.100	11.8	15.4	26.8	300	3.67	269	3.62

(b) Use of ice storage for cooling

To verify the system performance when the coolness stored in the form of ice is used for space cooling, 200 kg of ice is generated and kept in the storage tank. The ITES unit is now working with the main chilled water cycle. The base load is supported by the chilled-water cycle and the excess is supported by the ITES. Fig. 7 shows the simulated results and those from the experiments. Both agree quite well.

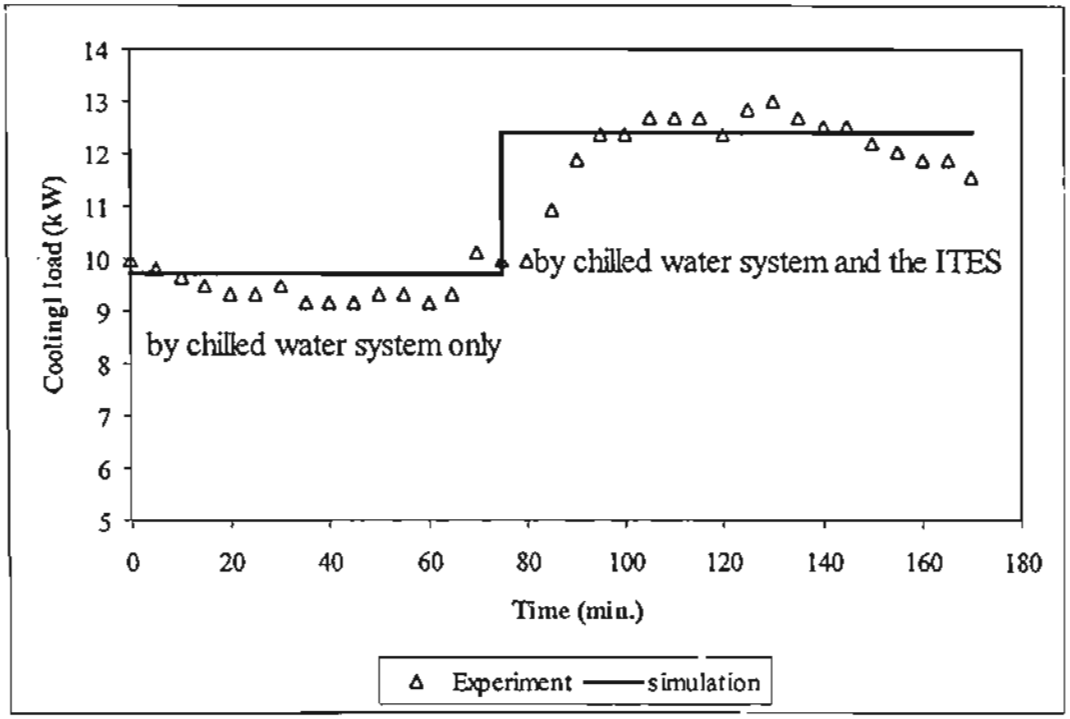

Fig. 7. Use of ice storage for cooling.

4.5 System Performance

In this section, the system performance is simulated to find out the appropriate working conditions. The results are illustrated in Figs. 8 and 9. As the refrigerant mass flow rate is varied for both cycles, the coefficient of performance (COP) of the chilled water system increases with the refrigerant mass flow rates. The highest value of COP is about 3.1 which is obtained when the refrigerant mass flow rate is about 0.08 kg/s and after that the COP slightly decreases. For the ice storage cycle, the cycle COP also depends on the compressor speed. Lower the compressor speed results in higher the COP. However, However, there is a limitation. The low compressor speed will shift the condensing temperature down. In the case of 7.1 rps compressor speed, the condensing temperature is approximately 21°C which is lower than the

average ambient temperature in Thailand, thus, 7.1 rps of the compressor speed is not acceptable. The refrigerant mass flow rate affects only slightly in the COP for higher compressor speed. The results are shown in Fig. 9.

To operate the appropriate conditions of chilled water cycle and the ice storage cycle, the recommended refrigerant mass flow rates are 0.07 – 0.09 kg/s for chilled water system and 0.08 – 0.09 kg/s which causes a short period of time to produce ice in the ITES. The compressor speed for the ITES system should be 9.5 rps due to the high value of COP.

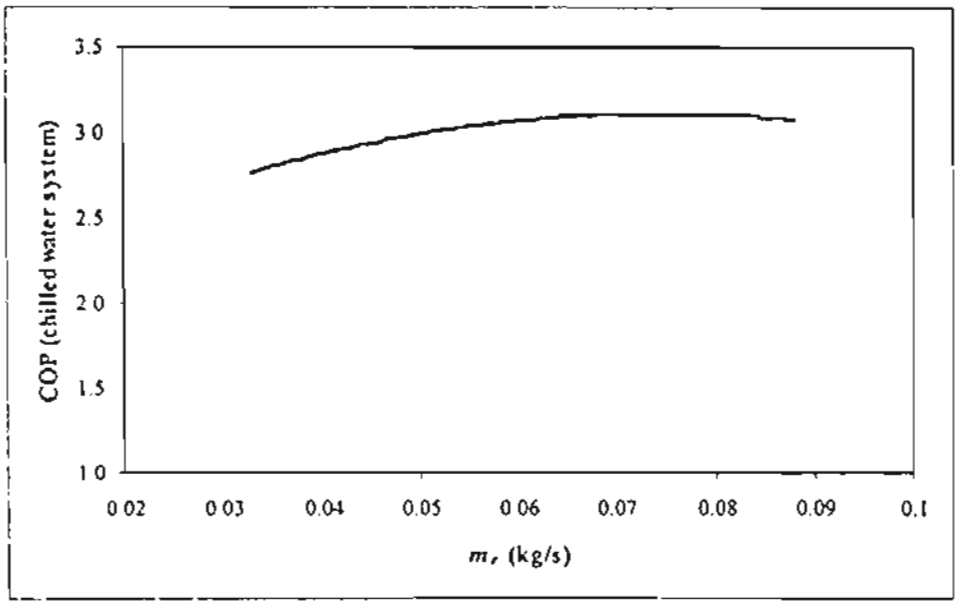

Fig. 8. COP of the chilled water system.

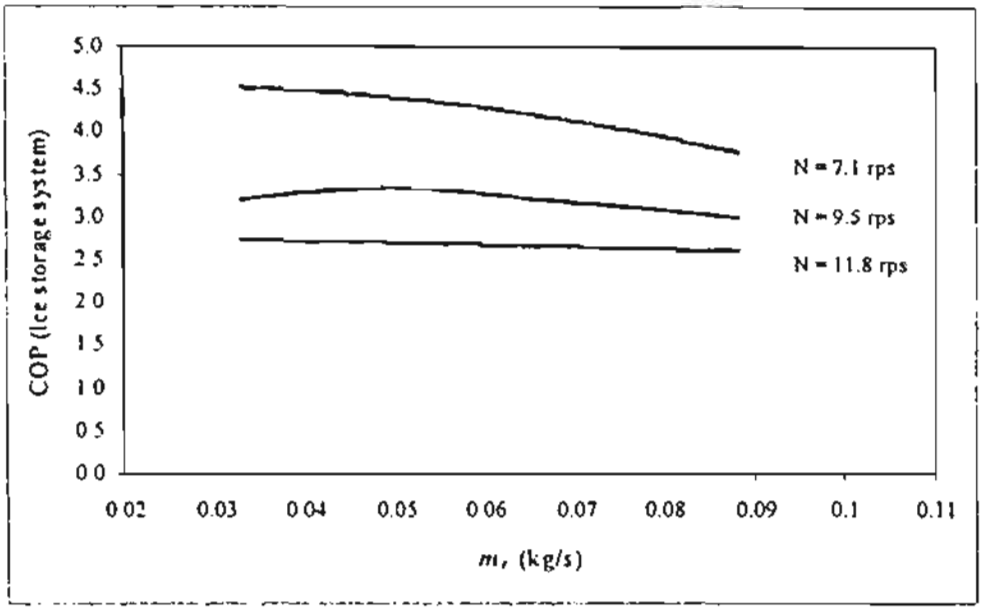

Fig. 9. COP of the ice storage system.

4. APPROPRIATE DESIGN OF THE ITES

In this section, the peak electrical energy demand (kW), energy consumption (kW-hr) and the electricity charge (Baht) for air conditioning system of each category are considered under the assumptions that

(1) The ice storage system is operated at 0.088 kg/s of refrigerant mass flow rate and 9.5 rps of compressor speed.

(2) The sufficient amount of the ice is produced and completely used in each day.

(3) The chilled water cycle is operated at full compressor speed. The refrigerant mass flow rate of the cycle is varied from 0.03 – 0.09 kg/s to support the base cooling load in each case.

The peak energy demand of the air conditioning system during on-peak period as shown in Table 3 is decreased when using the ITES unit assisted with the chilled-water cycle. As the cooling load is more supported by the ITES cycle, the peak energy demand is more reduced.

For categories 5 and 7, the time required for generating ice is longer than that of the off-peak period, therefore there is a load due to the compression mode of ITES cycle added up in the on-peak period. Higher energy consumptions are obtained compared with the conventional system(category 1).

Table 4 shows the electrical energy consumption of the air conditioning system in each category. Comparing to the conventional system (category: no storage), even the total energy consumed is nearly the same or higher, the energy consumed in the chilled-water system operating during the daytime is reduced by shifting the cooling load to the ITES system operating in the nighttime. The load factor will be more uniform.

Table 3. The peak energy demand at various categories on the design day.

Category	Peak energy demand caused by cooling and non-cooling system					Total peak demand of the office (kW)
	Chilled water system (kW)		ITES system (kW)		Non-cooling system (kW)	
	Off-peak (8 a.m. – 9 a.m.)	On-peak (9 a.m.- 5 p.m.)	Off-peak (10 p.m. – 8 a.m.)	On-peak	On-peak (1 p.m. – 4 p.m.)	On-peak (1 p.m. – 4 p.m.)
1	9.7	9.7	0	0	15	24.7
2	7.0	7.0	3.7	0	15	22.0
3	5.3	5.3	3.7	0	15	20.3
4	3.8	3.8	3.7	0	15	18.8
5	2.2	2.2	3.7	3.7 (8 am. – 9 a.m.)	15	17.2
6	3.3	3.3 (9 a.m.- 1 p.m.)	3.7	0	15	15.0
7	0	0	3.7	3.7 (8 a.m. – 10 a.m.)	15	15.0

Table 4. Energy consumed in air conditioning system during the year in each category.

Category	Energy consumption (kW-hr)		
	Chilled water system	ITES system	Total
1 (no storage)	13044.17	0	13044.17
2 (partial design, 25%)	12469.53	610.17	13079.71
3 (partial design, 40%)	10695.55	2965.58	13661.13
4 (partial design, 60%)	7838.09	7157.28	14995.37
5 (partial design, 80%)	4625.70	12152.30	16778.00
6 (demand-limited)	7046.39	6322.71	13369.10
7 (full storage)	0	16371.63	16371.63

The electricity charges of the office in both of the cooling system and non-cooling system are shown in Table 5. They includes the charge counted on the average maximum electricity used in kW over 15 minutes in each month (demand charge), the charge counted on the total amount of power consumed in kW-hr during each month (energy charge) and the service charge as shown in Table 1. As the peak demand reduced and the cooling load is more supported by the ITES system during the off-peak period, the demand charge and the energy charge of the office are reduced. However, due to the overlapped compressor load of the ITES in the on-peak period in the case of categories 5 and 7, the energy charge of the office is slightly increased. The load does not occur at the same time as the peak demand of the office, therefore, there is no effect on the demand charge.

The lowest total charge is obtained when the ITES system is designed as demand-limited in category 6.

Table 5. Electricity charge during the year in each category

Category	Electricity charge (Baht/year)			Total (Baht/year)
	Demand charge	Energy charge	Service charge	
1 (no storage)	30469.9	27301.1	4800	62571.0
2 (partial design, 25%)	27139.2	26878.4	4800	58817.6
3 (partial design, 40%)	25042.1	25579.0	4800	55421.1
4 (partial design, 60%)	23191.7	23750.9	4800	51742.6
5 (partial design, 80%)	21966.4	25782.2	4800	52548.6
6 (demand-limited)	18504.0	18099.1	4800	41403.1
7 (full storage)	18504.0	26297.88	4800	49703.4

The feasibility of using the ITES system with direct contact evaporator in this work is based on an adequate economic return of each storage option (partial, demand-limited and full storage) which has different investment and the maintenance costs. The profit of the ITES system is the decreased electricity charge comparing to the conventional system (1st category). The total electricity charges of all categories are also shown in Fig. 10. The payback periods of the ITES system of all categories are shown in Table 7. The discount rate is assumed to be 8% annually with 2.5% inflation. The most appropriate ITES in this study is the demand-limited storage design of which the limited peak demand is equal to maximum non-cooling demand of the office. In this case, the peak demand during the daytime from 24.7 kW in case of the conventional system could be reduced to 15 kW (39.3% decreased). The electricity charge of the office is reduced from 62,571 baht/year for conventional system to 41,403 baht/year resulting in 33.8% reduction. The payback period is 4.8 years which is the lowest in all categories.

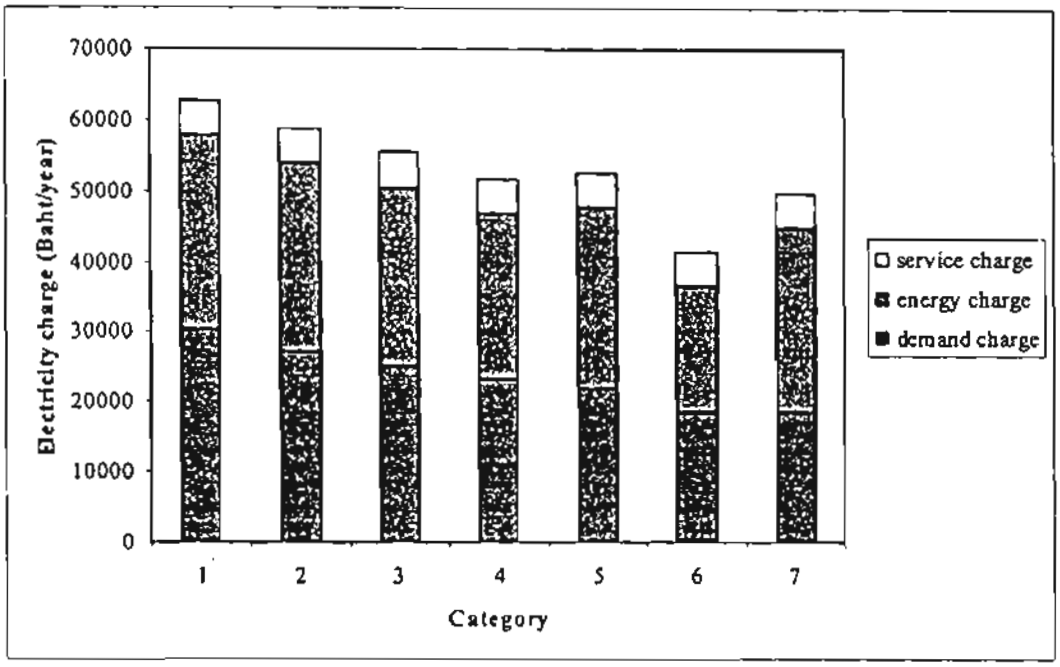

Fig. 10. Electricity charge during the year in each category.

Table 6. Incremental investment cost of the ITES system

Component Lists	Cost (Baht)
Compressor	15,000
Condensing unit	10,000
Direct contact evaporator tank	35,000
Nozzle	3,000
Compressor control motor	5,000
Piping and accessories for full storage design	3,000
Piping and accessories for partial storage design	3,500
Piping and accessories for demand-limited design	6,500
Control circuit for full storage design	1,500
Control circuit for partial storage design	2,500
Control circuit for demand-limited storage design	5,000
Salvage value of the conventional system for full storage design	-3,000
Total (full storage design)	69,500
Total (partial storage design)	74,000
Total (demand-limited storage design)	79,500

Table 7. Payback period of the ITES system at various categories.

Category	Incremental investment cost (Baht)	Decreasing electricity cost including maintenance cost (Baht/year)	Payback period (years)
1	0	0	0
2	74000	1753	More than 20 yrs.
3	74000	5150	More than 20 yrs.
4	74000	8828	11.4
5	74000	8022	13.1
6	79500	19168	4.8
7	69500	12970	6.0

CONCLUSION

The mathematical models of the main components in both of the chilled water system and the ice thermal energy storage with direct contact evaporator are formulated at various mass flow rates and compressor speed and the system performance has been simulated. The estimated values from the simulation program are in good agreement to the experimental results. The results from the simulation shows that the appropriate storage option of the ITES system for the selected office located in Chiang Mai University is the demand-limited design which could reduce the peak electricity demand of the office from 24.7 kW to 15 kW. The electricity charge of the office is also reduced from 62,571 baht/year for conventional system to 41,403 baht/year with the payback period is less than 5 years.

Acknowledgement – The authors gratefully acknowledge the support provided by Thailand Research Fund and the Joint Graduate School of Energy and Environment for carrying out this study.

REFERENCES

1. Electricity Generating Authority of Thailand (EGAT) (1997), *Thailand power development plan PDP 1997-01*. System Planning Department. Bangkok, Thailand.
2. Subbaiyer, S., Andhole, T.M. and Helmer, W.A. (1991), Computer Simulation of a Vapor-Compression Ice Generator with a Direct Contact Evaporator, *ASHRAE Transactions*, part 1, pp. 118-126, paper number 3448.
3. Wendland, R.M. (1990), Commercial Cool Storage, *Energy Engineering*, Vol. 87, No. 6, pp. 18-22.
4. Kiatsiriroat, T. and Maneechote, T. (1996). Formation and Melting of Ice with Direct contact Heat Exchange, paper presented in the *Tri-University International Joint Seminar & Symposium*, Jianxu University of Science & Technology, China.
5. Chatakanonda, T. and Na Bangchang, P. (1998), *A R22 Refrigeration Unit with Direct Contact Evaporator*. Senior Project, Mechanical Engineering, Chiang Mai University, Thailand.
6. Kiatsiriroat, T., Siriplubpla P. and Nuntaphan, A. (1998), Performance Analysis of a Refrigeration Cycle Using a Direct Contact Evaporator, *International Journal of Energy Research*, 22, pp. 1179-1190.
7. Kiatsiriroat, T., Chowcheun, K. and Wibulswas, P. (1994), Simulation of Standard Vapor Compression System, *ASEAN Journal on Science & Technology for Development*, 11(1), pp. 167-180.
8. Stoecker, W.F. (1982). *Refrigerant and Air Conditioning*. McGraw-Hill Book Company, New York, USA.
9. Mayhew, Y.R. and Rogers, G.F.C. (1972). *Thermodynamic and Transport Properties of Fluids*, Basil Blackwell, Oxford, U.K.

NOMENCLATURES

C_P	specific heat capacity (kJ/kgK)
h	specific enthalpy (kJ/kg)
k	polytropic index
L	latent heat (kJ/kgK)
m	mass flow rate (kg/s)
M	mass (kg)
N	compressor speed (rps)
P	pressure (MPa)
Q	heat transfer rate (kW)
T	temperature (°C)
Δt	period of time (s)
UA	overall heat transfer coefficient (kW/K)

Subscripts

a	air
amb	ambient
cd	condenser
ch	chiller
cp	compressor
ev	evaporator
ex	expansion valve
i	inlet
o	outlet
r	refrigerant
w	water

OUTPUT OF THE STUDY

1. Two Master Theses entitled:
    - An Ice Storage System Using a Direct Contact Evaporator for an Air – Conditioned Room, M.Eng Thesis, Department of Mechanical engineering, Chiang Mai University, 2000.
    - Development of a prototype of an ice thermal energy storage with direct contact evaporator, M.Phil Thesis, Joint Graduate School of Energy and Environment (JGSEE), King Mongkut's University of Technology, 2000.

2. Three published papers:
    - Energy Analysis of an Ice Thermal Energy Storage Prototype with Direct Contact Evaporator, Energy-The International Journal, Submitted.
    - Heat Transfer Model of a Direct a Direct Contact Evaporator, Applied Energy, Submitted.
    - Feasibility of Using Ice Thermal Energy Storage with Direct Contact Evaporator in an Office Building, Energy Research-The International Journal, Submitted.